LMTK3 represses tumor suppressor-like genes through chromatin remodeling in breast cancer

Article (Published Version)

Article

Cell Reports

LMTK3 Represses Tumor Suppressor-like Genes through Chromatin Remodeling in Breast Cancer

Graphical Abstract

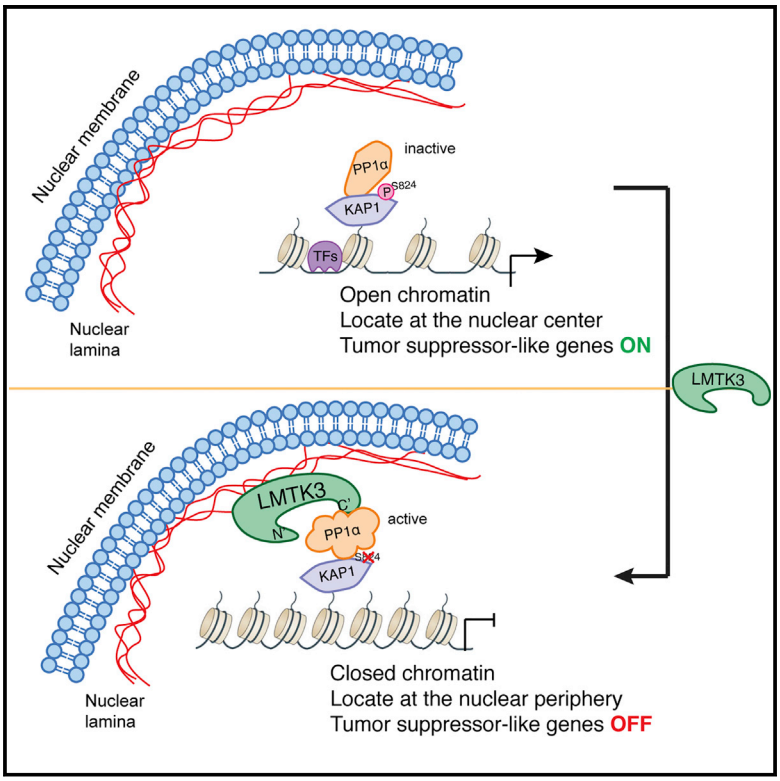

Authors

Yichen Xu, Hua Zhang, Van Thuy Mai Nguyen, ..., Luca Magnani, Justin Stebbing, Georgios Giamas

Correspondence

l.magnani@imperial.ac.uk (L.M.), g.giamas@imperial.ac.uk (G.G.)

In Brief

Xu et al. describe a kinase-independent role of LMTK3 in transcriptional regulation. The authors find that the scaffolding properties of LMTK3 are responsible for chromatin remodeling and its tethering to the nuclear lamina. These dynamic events result in repression of LMTK3-bound tumor suppressor-like genes, further supporting the oncogenic role of LMTK3.

Highlights

- LMTK3 can act as a DNA binding protein that represses tumor suppressor-like genes
- LMTK3 mediates chromatin condensation
- LMTK3 tethers the chromatin to the nuclear periphery

Accession Numbers

GSE70385

Xu et al., 2015, Cell Reports *12*, 1–13
August 4, 2015
http://dx.doi.org/10.1016/j.celrep.2015.06.073

CellPress

Please cite this article in press as: Xu et al., LMTK3 Represses Tumor Suppressor-like Genes through Chromatin Remodeling in Breast Cancer, Cell Reports (2015), http://dx.doi.org/10.1016/j.celrep.2015.06.073

Cell Reports
Article

LMTK3 Represses Tumor Suppressor-like Genes through Chromatin Remodeling in Breast Cancer

Yichen Xu,[1] Hua Zhang,[1] Van Thuy Mai Nguyen,[1] Nicos Angelopoulos,[1] Joao Nunes,[1] Alistair Reid,[1] Laki Buluwela,[1] Luca Magnani,[1,2,*] Justin Stebbing,[1,2] and Georgios Giamas[1,2,*]
[1]Division of Cancer, Imperial College London, Department of Surgery and Cancer, Hammersmith Hospital Campus, Du Cane Road, London W12 0NN, UK
[2]Co-senior author
*Correspondence: l.magnani@imperial.ac.uk (L.M.), g.giamas@imperial.ac.uk (G.G.)
http://dx.doi.org/10.1016/j.celrep.2015.06.073

SUMMARY

LMTK3 is an oncogenic receptor tyrosine kinase (RTK) implicated in various types of cancer, including breast, lung, gastric, and colorectal cancer. It is localized in different cellular compartments, but its nuclear function has not been investigated so far. We mapped LMTK3 binding across the genome using ChIP-seq and found that LMTK3 binding events are correlated with repressive chromatin markers. We further identified KRAB-associated protein 1 (KAP1) as a binding partner of LMTK3. The LMTK3/KAP1 interaction is stabilized by PP1α, which suppresses KAP1 phosphorylation specifically at LMTK3-associated chromatin regions, inducing chromatin condensation and resulting in transcriptional repression of LMTK3-bound tumor suppressor-like genes. Furthermore, LMTK3 functions at distal regions in tethering the chromatin to the nuclear periphery, resulting in H3K9me3 modification and gene silencing. In summary, we propose a model where a scaffolding function of nuclear LMTK3 promotes cancer progression through chromatin remodeling.

INTRODUCTION

Lemur tyrosine kinase 3 (LMTK3), a member of the receptor tyrosine kinase family (RTK), has been identified previously as an estrogen receptor α (ERα) regulator (Giamas et al., 2011) implicated in endocrine resistance in breast cancer (Stebbing et al., 2013). However, LMTK3 is expressed in both ERα$^+$ and ERα$^-$ breast cancers, suggesting that it plays different cellular roles independent of ERα status. Our recent work has revealed that elevated cytoplasmic LMTK3 abundance in triple-negative breast cancer promotes tumor invasion and metastasis (Xu et al., 2014), which provided an example of the ERα-independent action of LMTK3. Interestingly, both nuclear and cytoplasmic expression of LMTK3 are correlated with tumor grade and patient survival (Stebbing et al., 2012). However, the exact function of the nuclear LMTK3 has not been determined so far.

Several receptor tyrosine kinases (RTKs) have been reported to localize in the nucleus, where they can regulate gene expression (most likely transactivation) through binding to euchromatin (Hung et al., 2008; Lin et al., 2001; Lo et al., 2005; Peng et al., 2001; Wang et al., 2004). According to these reports, nuclear RTKs are present in the nucleoplasm instead of the nuclear lamina. In most cells, at least one class of heterochromatin is positioned at the nuclear lamina, resulting in gene repression (Andrulis et al., 1998; Finlan et al., 2008; Guelen et al., 2008; Kumaran and Spector, 2008; Peric-Hupkes et al., 2010; Reddy et al., 2008; Solovei et al., 2013; Towbin et al., 2012). Previous studies also propose that heterochromatin relocation to the nuclear lamina might occur via active tethering mediated by discrete molecular complexes (Chubb et al., 2002; Poleshko et al., 2013). These perinuclear heterochromatin hotspots are enriched with histone 3 lysine 9 dimethylation (H3K9me2) and trimethylation (H3K9me3) modifications, which are usually associated with a number of heterochromatin binding proteins such as KRAB-associated protein 1 (KAP1/TIF1β/TRIM28), a binding partner of histone-lysine N-methyltransferase SETDB1 (Grewal and Jia, 2007; Nielsen et al., 1999; Ryan et al., 1999; Zeng et al., 2010).

KAP1 is a transcriptional co-repressor whose activity is regulated by post-translational modifications such as phosphorylation and sumoylation. When phosphorylated, KAP1 affects global chromatin decondensation (Ziv et al., 2006), which, in turn, results in the derepression of KAP1-bound genes such as those involved in cell-cycle arrest and apoptosis (Lee et al., 2007; Li et al., 2007). It has been shown that KAP1 phosphorylation is regulated by protein phosphatases 1α (PP1α) and 1β (PP1β), which are responsible for the maintenance of its repressive function (Li et al., 2010).

In this study, we investigate the function of nuclear LMTK3 through mapping genome-wide chromatin interaction sites of LMTK3 in breast cancer. We find that LMTK3 suppresses the expression of tumor suppressor-like genes by tethering the chromatin to the nuclear periphery, functioning as a catalytic scaffold protein. Binding of LMTK3 to chromatin is mediated via the interaction with PP1α and KAP1. The formation of this complex leads to the suppression of KAP1 phosphorylation, in turn strengthening this unique transcriptional repression function. We show that a protein kinase has scaffolding properties, creating a system to enhance signaling complexity in carcinogenesis.

Please cite this article in press as: Xu et al., LMTK3 Represses Tumor Suppressor-like Genes through Chromatin Remodeling in Breast Cancer, Cell Reports (2015), http://dx.doi.org/10.1016/j.celrep.2015.06.073

RESULTS

Genome-wide Mapping Identifies the LMTK3-Chromatin Binding Profile

We have previously identified LMTK3 as a potential therapeutic target in breast cancer that is expressed in ERα$^+$ and ERα$^-$ breast cancer, whose expression carries prognostic significance in both subgroups. As shown previously (Xu et al., 2014), two specific LMTK3 bands are detected by western blot analysis. We now demonstrate that LMTK3 localizes both in the nucleus and in the cytoplasm of MCF7 and MDA-MB-231 cells. The upper band is specifically localized in the cytoplasm, and the lower band is detected both in the cytoplasm and in the nucleus, which suggests that the lower band is the one that mainly functions in the nucleus (Figures S1A and S1B). Because the importin protein family is known to mediate macromolecules translocation from the cytoplasm to the nucleus (Weis, 2003), we decided to investigate whether importins are responsible for LMTK3 translocation by knocking down importin α2 and importin β1 individually. We detected a notable reduction in nuclear LMTK3 levels, with an increase in its cytoplasmic proportion after importin α2 but not importin β1 knockdown (Figure S1C), suggesting that LMTK3 translocation is mediated in an importin α2-dependent/importin β1-independent manner, which has also been reported previously (Kotera et al., 2005).

To decipher the function of LMTK3 in the nucleus, we mapped the genome-wide profile of LMTK3-chromatin interactions by chromatin immunoprecipitation sequencing (ChIP-seq) in the ERα$^+$/MCF7 and the ERα$^-$/MDA-MB-231 cell lines. We observed 3,086 loci in MCF7 and 24,516 loci in MDA-MB-231, in which LMTK3 is located to the chromatin (Figures S1D and S1E).

Based on our previous work showing that LMTK3 interacts with and phosphorylates ERα, which, in turn, promotes *TFF1* expression (Giamas et al., 2011), we questioned whether LMTK3-chromatin binding events are ERα-dependent. Interestingly, we observed that LMTK3 binding in MCF7 (ERα$^+$) and MDA-MB-231 (ERα$^-$) have a high similarity (Figures 1A and S1D) with a high correlation (R^2 = 0.77) (Figure 1B). Supporting the notion that chromatin-bound LMTK3 function may be independent of ERα, we found no noticeable overlap and correlation between LMTK3 and ERα binding (Figures S1F and S1G). Moreover, there were no significant changes in the enrichment of selected LMTK3 binding genes in MCF7 cells upon fulvestrant-mediated ERα degradation (Figure S1H), further suggesting that the DNA binding events of LMTK3 are ERα-independent. To further characterize the LMTK3 binding behavior, we then tested the correlation of binding events of LMTK3 with two groups of chromatin biomarkers (histone and transcription factors [TFs]): repressive promoter markers (histone 3 lysine 27 trimethylation [H3K27me3], H3K9me3, and SUZ12) and active promoter or enhancer markers (histone 3 lysine 4 monomethylation [H3K4me1], histone H3 lysine 4 trimethylation [H3K4me3], NANOG, p300, and TAF1). Interestingly, we found that LMTK3 binds chromatin at both repressive and active (Figures 1C, 1D, and S1I) promoters, suggesting that there is a different binding profile of LMTK3 compared with the ones of other known RTKs (Lin et al., 2001; Wang et al., 2004).

Next, we validated LMTK3 bindings using ChIP-qPCR for the most enriched LMTK3-binding genes. To confirm that the bindings are LMTK3-specific, we constructed stable LMTK3 knockout (KO) MDA-MB-231 cells using a clustered regularly interspaced short palindromic repeats (CRISPR)/CAS9 technique by transfecting MDA-MB-231 cells with plasmids containing hCAS9 and 2 guiding RNAs targeting exon 12 of LMTK3. Positive clones showed a 112-base pair (bp) deletion (Figure S1J), and clones with significant LMTK3 protein deletion were selected (Figure S1K). Interestingly, we could not generate complete LMTK3 KO MCF7 cells using the CRISPR technique. This may be due to the fact that LMTK3 is so crucial for MCF7 cell growth that LMTK3 KO cell clones stopped proliferating and could not be selected. Therefore, we used our previously established MCF7 cells stably overexpressing LMTK3 (MCF7-LMTK3). As a result, LMTK3 binding events were notably higher in MCF7-LMTK3 cells compared with MCF7 cells (Figure 1E) and were barely detected in LMTK3-KO MDA-MB-231 cells (Figure 1F), suggesting that the bindings detected are LMTK3-specific.

To investigate the binding event of LMTK3 in vivo, we injected MCF7-LMTK3 cells subcutaneously into nude mice, harvested the tumors, and performed LMTK3 ChIP. We discovered a similar binding pattern of LMTK3 in the xenograft studies compared with that in cell lines (Figure 1G). Finally, we also confirmed LMTK3 bindings in both ERα$^+$ and ERα$^-$ breast cancer patient samples (Figure 1H). In summary, our results highlight that nuclear LMTK3 is a chromatin-binding protein whose activity is independent of ERα status.

Motif and RIME Analyses Identify KAP1 as an LMTK3-Associated Protein in Chromatin Binding

Similar to other RTKs, LMTK3 is unlikely to have a DNA-binding domain. Therefore, binding of LMTK3 at DNA requires sequence-specific transcription factors that interact with LMTK3. A motif analysis provided a number of potential interacting partners of LMTK3 (Figure 2A). We performed rapid immunoprecipitation mass spectrometry of endogenous proteins (RIME) (Mohammed et al., 2013) to further address which of these candidates might be interacting partners of LMTK3 during DNA binding and discovered 196 LMTK3-associated proteins (Figures 2B and S2; Table S1). Interestingly, KAP1 was enriched in both analyses. We validated the interaction between LMTK3 and KAP1 by immunoprecipitation (Figure 2C). In addition, we found a notable correlation between global LMTK3 and KAP1 binding events by comparing the ChIP-seq signals of LMTK3 and KAP1 (from the HEK293 cell line) (Figure 2D). We further confirmed KAP1 as an LMTK3-binding partner by performing KAP1 re-ChIP after LMTK3 ChIP (Figure 2E). In addition, we also detected a similar binding profile of LMTK3 and KAP1 (Figure 2F). These data substantiate that KAP1 is an LMTK3 binding partner in chromatin binding.

PP1α Stabilizes the LMTK3/KAP1 Interaction and Mediates KAP1 Dephosphorylation at LMTK3-KAP1-Bound Chromatin Regions, Resulting in Chromatin Condensation and Gene Repression

We then investigated whether the LMTK3/KAP1 interaction is a kinase-substrate process. No phosphorylation was observed

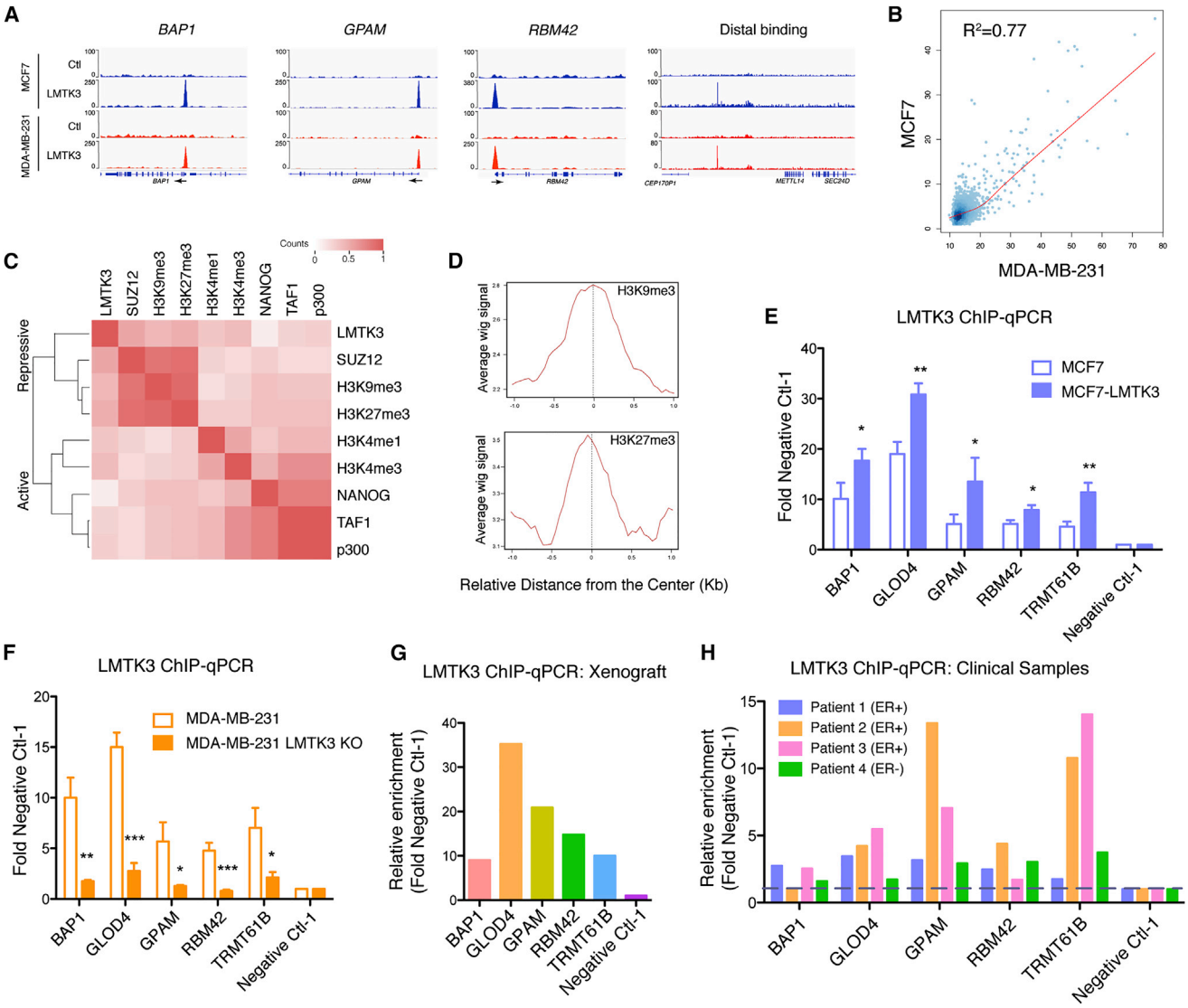

Figure 1. Identification of Genome-wide LMTK3 Binding Sequences with ChIP-Seq

(A) Binding of LMTK3 at the promoter of *BAP1*, *GPAM*, *RBM42*, and the distal interval in MCF7 and MDA-MB-231 cells.

(B) The correlation of LMTK3 binding signals in the MCF7 and MDA-MB-231 breast cancer cell lines.

(C) Clustering of genome-wide binding datasets with LMTK3. The color indicates similarity based on the Pearson correlation of the ChIP-seq peaks. The R^2 values of the correlation between LMTK3 bindings and SUZ12, H3K9me3, H3K27me3, H3K4me1, H3K4me3, NANOG, TAF1, and p300 binding are 0.53, 0.41, 0.48, 034, 0.4, 0.11, 0.26, and 0.27, respectively.

(D) H3K9me3 and H3K27me3 enrichment around LMTK3 peaks in MCF7 cells.

(E and F) ChIP-qPCR of LMTK3 bindings in MCF7 and MCF7-LMTK3 (E) and MDA-MB-231 and LMTK3 KO MDA-MB-231 cells (F).

(G) ChIP-qPCR of LMTK3 binding in an MCF7-LMTK3 cell-implanted xenograft.

(H) ChIP-qPCR of LMTK3 binding in human breast cancer tissues. Patient 1, ER^+ PR^+ $HER2^-$; patient 2, ER^+, HER^-; patient 3, ER^+, PR^+, HER^-; patient 4, ER^- PR^- $HER2^+$.

Quantitative data are presented as mean ± SD from three experiments. *p < 0.05, **p < 0.01, ***p < 0.001. See also Figure S1.

after performing an in vitro kinase assay using the recombinant LMTK3 kinase domain (encompassing amino acids [aas] 149-444) as a source of enzyme activity and glutathione S-transferase (GST)-KAP1 as a substrate (Figure S3A). On the contrary, endogenous KAP1 phosphorylation at Ser824 was suppressed after LMTK3 overexpression (Figures S3B and S3C). Because PP1α is a known KAP1 phosphatase and a predicted LMTK3 interaction partner (Hendrickx et al., 2009), we tested whether PP1α is involved in the LMTK3/KAP1 interaction. Interestingly, silencing of PP1α reduced the interaction between LMTK3 and KAP1 (Figure 3A). We therefore generated GST-LMTK3 constructs and LMTK3 mutations at the PP1α docking motif (PP1_RVxF) of LMTK3 (Figure 3B). As anticipated, a significant decrease in LMTK3-PP1α binding was detected in both mutants

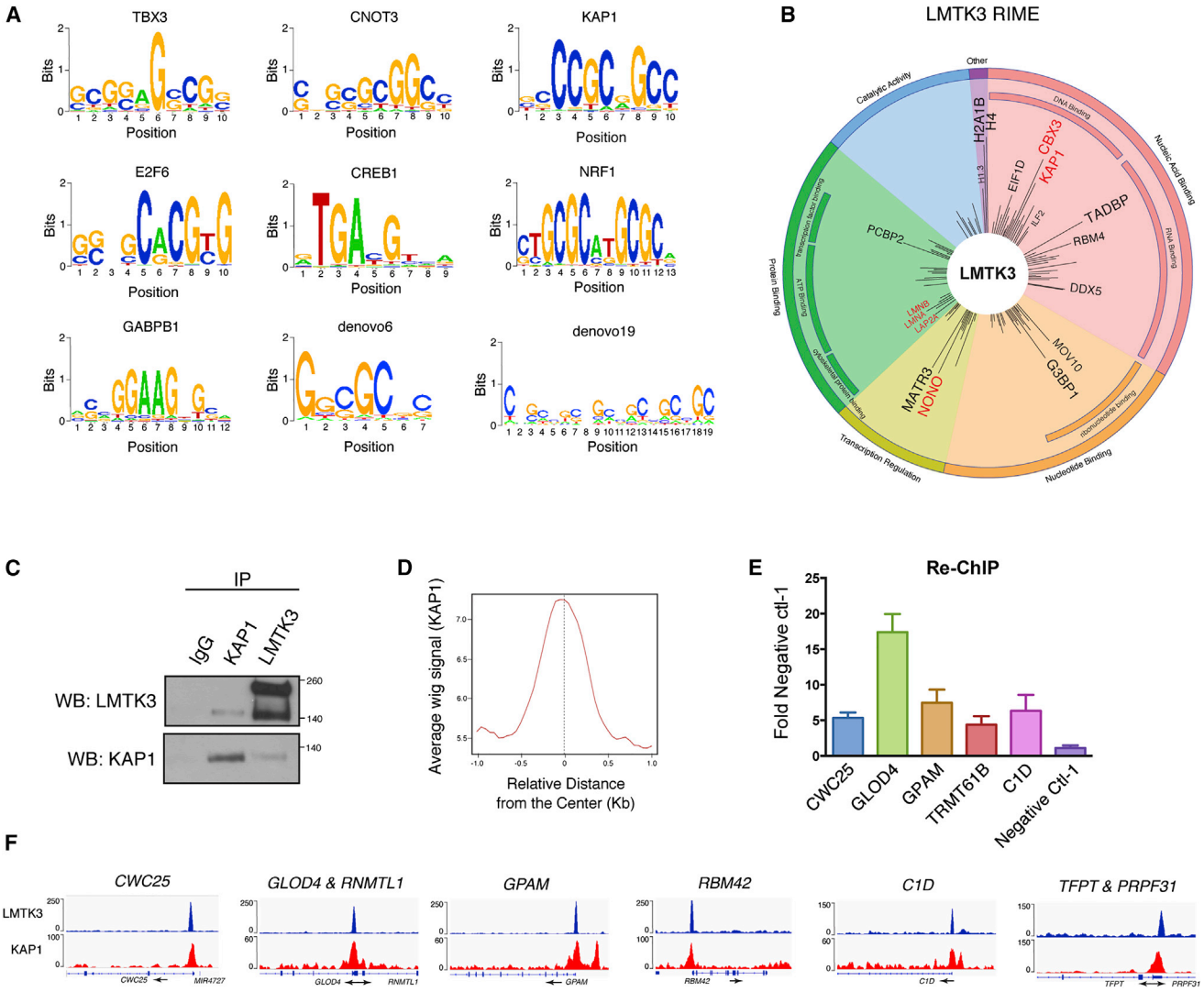

Figure 2. KAP1 Is an Interacting Partner of LMTK3 in Chromatin Binding

(A) Selected examples of conserved TF motifs enriched within the interval regions associated with LMTK3.

(B) LMTK3 RIME in MCF7 cells identified potential LMTK3-associated proteins in DNA binding.

(C) Western blotting (WB) showing the immunoprecipitation (IP) of LMTK3 and KAP1 in MCF7 cells.

(D) KAP1 enrichment around LMTK3 peaks.

(E) qPCR results showing re-ChIP experiments using a KAP1 antibody after LMTK3 ChIP.

(F) Examples of LMTK3-KAP1 overlap based on snapshots of ChIP-seq data for the indicated genes.

See also Figure S2 and Table S1.

(LMTK3^{RVxF_1} and LMTK3^{RVxF_2}), with a subsequent reduction in the LMTK3/KAP1 interaction (Figures 3B and 3C). These results suggest that PP1α is crucial for stabilizing the LMTK3-KAP1 complex.

KAP1 phosphorylation is critical in global chromatin decondensation (White et al., 2006; Ziv et al., 2006), leading to the derepression of several basal KAP1-repressed genes (Lee et al., 2007; Li et al., 2007). Therefore, we were interested in elucidating the function of the LMTK3-PP1α-KAP1 interaction on KAP1 phosphorylation status as well as its repressive function. Because basal levels of KAP1 phosphorylation are barely detected, we used doxorubicin, a KAP1-Ser824 phosphorylation inducer, as a molecular tool to study the LMTK3-PP1α-KAP1 effect on KAP1 phosphorylation. We further discovered that silencing *PPP1CA* (a PP1α-encoding gene) rescued the reduced Ser824 phosphorylation of KAP1 in MCF7-LMTK3 cells (Figure 3D), indicating that LMTK3 requires PP1α to dephosphorylate KAP1. Silencing of PP1β, however, did not rescue the reduced phosphorylation of KAP1 induced by LMTK3 (Figure S3D). Interestingly, we noticed that there was no increase in KAP1 and PP1α interaction after LMTK3 overexpression (Figure S3E), suggesting that LMTK3 might promote PP1α

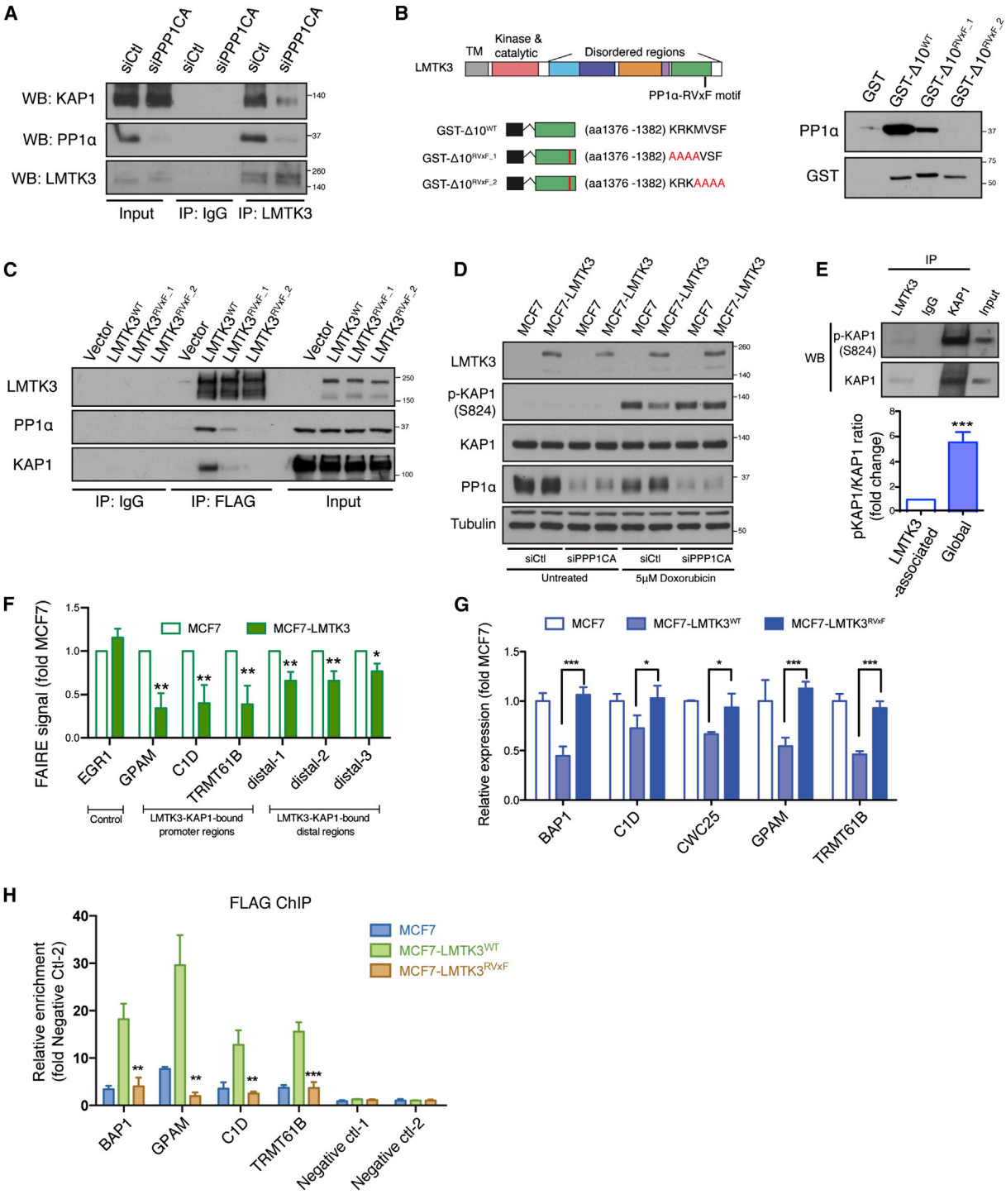

Figure 3. PP1α Stabilizes the LMTK3/KAP1 Interaction and Suppresses KAP1 Phosphorylation on Ser824 at LMTK3-Binding Regions

(A) Immunoprecipitation of KAP1 and PP1α with LMTK3 in MCF7 cell lysates with and without PPP1CA silencing for 72 hr.

(B) Left: schematic of the PP1α-interacting motif (RVxF motif) on LMTK3 and the indicated GST constructs. Right: GST pull-down of PP1α using a wild-type LMTK3 construct (GST-Δ10^{WT}) and two RVxF motif mutants (GST-Δ10^{RVxF_1} and GST-Δ10^{RVxF_2}). TM, transmembrane.

(C) FLAG immunoprecipitation performed after 24 hr of transient overexpression of FLAG-LMTK3^{WT} and two mutants (FLAG-LMTK3^{RVxF_1} and FLAG-LMTK3^{RVxF_2}).

(D) Western blotting of the indicated proteins in MCF7 and MCF7-LMTK3 cells transfected with PPP1CA small interfering RNA (siRNA) for 72 hr and treated with doxorubicin for 1 hr.

(legend continued on next page)

Please cite this article in press as: Xu et al., LMTK3 Represses Tumor Suppressor-like Genes through Chromatin Remodeling in Breast Cancer, Cell Reports (2015), http://dx.doi.org/10.1016/j.celrep.2015.06.073

dephosphorylation on KAP1 through increasing PP1α activity rather than its interaction with KAP1.

We further questioned whether the reduced KAP1 phosphorylation is predominantly observed at LMTK3-bound regions and whether this would result in chromatin condensation. To clarify this, we performed LMTK3 and KAP1 immunoprecipitation using chromatin-bound MCF7-LMTK3 cell lysates. The ratio of pKAP1/KAP1 in the LMTK3 immunoprecipitated chromatin complex is significantly lower than that in the KAP1 immunoprecipitated chromatin complex (Figure 3E), suggesting that LMTK3 suppresses KAP1 phosphorylation specifically at LMTK3-bound regions. Moreover, open chromatin is more enriched in MCF7 compared with MCF7-LMTK3 cells (Figure 3F), suggesting that the region-specific dephosphorylation of KAP1 by LMTK3 could suppress chromatin decondensation. Then we tested whether LMTK3/PP1α/KAP1-mediated chromatin condensation can lead to gene silencing. Overexpression of wild-type (WT) LMTK3, but not the mutant that abolishes its interaction with PP1α and KAP1 ($LMTK3^{RVxF\_2}$), suppresses indicated gene expression (Figure 3G) because of the fact that the latter lost the DNA-binding activity at these regions (Figure 3H). In summary, these results demonstrate that an LMTK3-PP1α interaction suppresses KAP1 phosphorylation, resulting in chromatin condensation and transcriptional repression.

LMTK3 and KAP1 Suppress Gene Expression at Distal Regions by Tethering Chromatin to the Nuclear Periphery

To decipher the function of LMTK3 chromatin binding, we separated LMTK3 and KAP1 binding events into promoter regions that are 1 kb preceding the transcription starting site and the rest as distal intervals. A recent study has suggested that KAP1 is highly associated with H3K9me3-marked heterochromatin (Bartke et al., 2010), (Iyengar et al., 2011; Vogel et al., 2006) and interacts with lamin A, a well characterized constituent of the nuclear lamina (Roux et al., 2012) that is associated with inactive chromatin regions (Kind et al., 2013; Peric-Hupkes et al., 2010; Sadaie et al., 2013). Despite the function of LMTK3 in chromatin condensation and transcriptional silencing, we found that distal intervals bound by LMTK3 (or KAP1) are associated with H3K9me3 modifications (Figure S4A). We therefore investigated the role of LMTK3 and KAP1 distal binding in the context of transcriptional repression. We discovered, using confocal microscopy, that LMTK3 (Figure 4A) and KAP1 (Figure S4B) co-localize with H3K9me3 both in the center and at the inner nuclear membrane. Studies have shown that gene transcription is suppressed when H3K9me3-marked heterochromatin is tethered to the nuclear periphery (Finlan et al., 2008; Reddy et al., 2008; Towbin et al., 2012). Therefore, we investigated whether LMTK3 and KAP1 are implicated in this process. When KAP1 was silenced, we noticed a partial loss of H3K9me3 staining on the inner nuclear membrane (Figure S4C). Similarly, we found that overexpression of LMTK3 significantly increased the proportion of H3K9me3 heterochromatin staining on the periphery (Figure 4B) compared with control cells, whereas LMTK3 deletion in MDA-MB-231 cells had the opposite effect (Figure S4D), suggesting that LMTK3 and KAP1 are involved in the heterochromatin repositioning process. To clarify whether LMTK3 interacts with the nuclear lamina, we used a series of GST-LMTK3 truncated protein constructs (Figure 4C) and performed in vitro GST pull-down assays. Notably, part of the structurally disordered domains of LMTK3 (Δ3 and Δ4) were found to interact with lamin A (Figure 4C), suggesting that LMTK3 may function as a scaffold protein inducing heterochromatin repositioning at the nuclear periphery by interacting with Lamin A. Interestingly, we also detected a significant overlap of LMTK3 distal binding regions with lamin-associated domains (LADs) (Guelen et al., 2008), supporting the hypothesis that LMTK3-associated regions are located at and interact with the nuclear lamina (Figure 4D). In aggregate, these results suggest that the LMTK3-KAP1 complex appears to be involved in tethering heterochromatin to the nuclear periphery.

To detect the sub-nuclear localization of the specific genomic regions bound by LMTK3, we performed DNA fluorescence in situ hybridization (FISH) with bacterial artificial chromosome (BAC) probes mapped to genomic regions where LMTK3 bound. We found an increase in FISH signals of the LMTK3-bound region (RP11-54O14) detected at the nuclear periphery when LMTK3 was overexpressed, whereas no significant change was observed in the non-LMTK3-bound region (RP11-113M21) (Figure 4E). The H3K9me3 signal was mostly increased upon LMTK3 overexpression at these regions, presenting a significant association with the increased FISH signals (Figure 4F).

To extend these observations and evaluate the transcriptional effect of active localization of the LMTK3-bound regulatory region to the nuclear periphery, we analyzed the expression patterns of genes around LMTK3 distal binding regions with RNA sequencing (RNA-seq) data. We chose the genes located near the distal intervals bound by LMTK3 (potential nuclear lamina anchors) and separated them into three groups: less than 100 kb (<100 kb) (18 genes), between 100 and 200 kb (100∼200 kb) (14 genes), and between 200 and 500 kb (200∼500kb) (39 genes) distance from LMTK3 binding sites (Figure 4G). We then compared the expression levels of the groups according to their expression values from RNA-seq. Notably, the expression levels of genes that are more distant from LMTK3 binding sites (100∼200 kb and 200∼500 kb) were relatively higher (Figure 4H). Interestingly, we detected a limited number of genes near LMTK3 distal binding sites. This can be explained by the fact that LMTK3 binding regions are highly associated with

(E) Immunoprecipitation of p-KAP1 (Ser824) and KAP1 with LMTK3 and KAP1 using chromatin-bound MCF7-LMTK3 cell lysate (upper panel). LMTK3- (LMTK3-associated) and KAP1-immunoprecipitated (Global) p-KAP1/KAP1 ratios are shown (lower panel).
(F) Formaldehyde-assisted isolation of regulatory elements (FAIRE)-qPCR in MCF7 and MCF7-LMTK3 cells at the indicated regions.
(G) qPCR of LMTK3-bound gene expression in MCF7, MCF7-$LMTK3^{WT}$, and MCF7-$LMTK3^{RVxF}$ cells.
(H) FLAG ChIP-qPCR of LMTK3-bound chromatin regions in MCF7-$LMTK3^{WT}$ and MCF7-$LMTK3^{RVxF}$ (FLAG-tagged) cells.
Quantitative data are presented as mean ± SEM from three experiments. Student's t test was used for statistical analysis. *$p < 0.05$, **$p < 0.01$, ***$p < 0.001$. See also Figure S3.

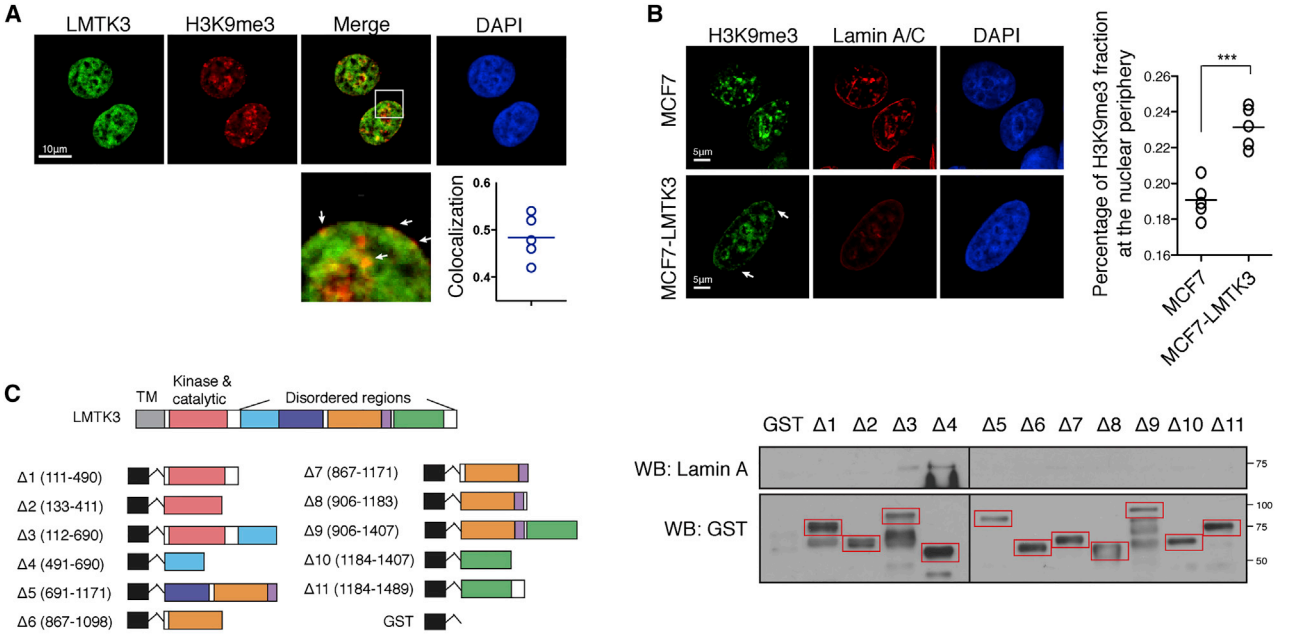

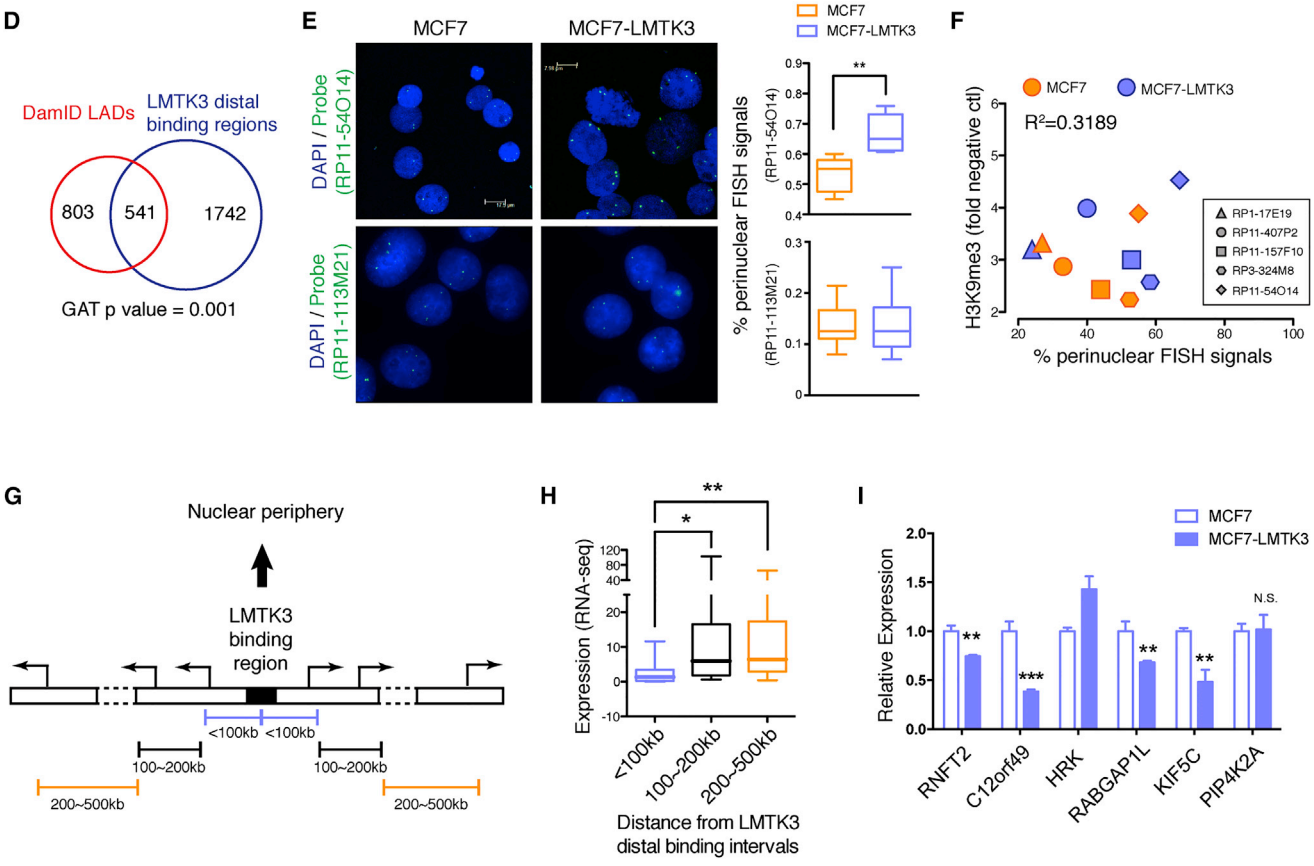

Figure 4. Distally Binding LMTK3 Tethers H3K9me3-Marked Heterochromatin to the Nuclear Periphery and Suppresses Nearby Gene Expression

(A) Confocal staining of LMTK3 and H3K9me3 in MCF7 cells. DAPI, 4′,6-diamidino-2-phenylindole.

(B) Confocal staining of H3K9me3 and Lamin A/C in MCF7 and MCF7-LMTK3 cells. H3K9me3 signals at the nuclear periphery were quantified.

(legend continued on next page)

Please cite this article in press as: Xu et al., LMTK3 Represses Tumor Suppressor-like Genes through Chromatin Remodeling in Breast Cancer, Cell Reports (2015), http://dx.doi.org/10.1016/j.celrep.2015.06.073

lamin-associated domains that were found to be gene-poor regions (Guelen et al., 2008; Meuleman et al., 2013; Peric-Hupkes et al., 2010; Pickersgill et al., 2006). We also confirmed that LMTK3 might suppress nearby gene expression by testing the expression of certain genes near LMTK3 distal regions (Figure 4I). This implies that LMTK3 binding at distal regulatory regions may be involved in suppressing nearby gene expression through tethering the heterochromatin to the nuclear periphery.

LMTK3, PP1α, and KAP1 Are Co-expressed in Breast Cancers and Collaborate in Suppressing the Expression of Tumor Suppressor-like Genes

To examine the clinical implication of transcriptional repression because of LMTK3 DNA binding, we chose the top LMTK3 and KAP1 binding genes at the promoter intervals and the top genes near the distal intervals and tested the clinical correlation of their mean expression levels and relapse-free survivals (RFSs) in breast cancer patients. A lower expression of genes bound by LMTK3 at promoter intervals (Figure 5A) and genes near LMTK3 bindings at the distal intervals (Figure 5B) were correlated with poorer RFS, suggesting that LMTK3-bound genes behave like tumor suppressor genes.

We also found that *LMTK3* expression is negatively correlated with the expression of several LMTK3-bound genes in breast cancer patient samples (The Cancer Genome Atlas [TCGA] database). As examples, the expression of *LMTK3* is negatively correlated with that of *GPAM* (Figure 5C) and *RABGAP1L* (Figure 5D), which are LMTK3-bound genes at promoter and distal intervals, respectively. This supports the hypothesis that LMTK3 directly regulates the transcription of LMTK3-bound genes in vivo as well as in our cell lines models.

In agreement with previous studies, *LMTK3* is significantly overexpressed in breast cancer (Figure 5E). Therefore, we decided to investigate the clinical impact of the LMTK3 binding partners KAP1 and PP1α. *KAP1* and *PPP1CA* are significantly overexpressed in breast tumors compared with normal tissues (Figure 5E, S5A, and S5B). In addition, high expression of *KAP1* and *PPP1CA* is associated with worse patient RFS (Figures 5F and 5G) and overall survival (Figures S5C and S5D). We also questioned whether *LMTK3*, *PPP1CA*, and *KAP1* co-express in breast cancer. Our analyses revealed a positive correlation between the expression of *LMTK3* and *KAP1* (Figure 5H), *LMTK3* and *PPP1CA* (Figure 5I), as well as *KAP1* and *PPP1CA* (Figure 5J) but not *LMTK3* and *PPP1CB* (Figure S5E) in patient samples (TCGA). These suggest that LMTK3, PP1α, and KAP1 collaborate in breast cancer progression, leading to poorer survival rates by inhibiting a number of tumor suppressor-like genes.

DNA-Binding Activity Is Crucial for LMTK3-Mediated Tumor Growth In Vitro and In Vivo

We also investigated whether the previously described proliferation advantage of LMTK3 in MCF7 cells (Xu et al., 2014) is ERα-mediated. We observed that, upon ERα removal via fulvestrant treatment, the proliferation of both MCF7 and MCF7-LMTK3 cells was significantly suppressed. However, in the absence of ERα, MCF7-LMTK3 cells could still proliferate faster than MCF7 cells (Figure S6A). Moreover, knockout of LMTK3 in the ERα^{-} MDA-MB-231 cells resulted in a slight but statistically significant reduction in cell proliferation (Figure S6B). Taken together, these results suggest that the involvement of LMTK3 in cell growth could partly depend on ERα but can also be subject to its transcriptional repression of tumor suppressor-like genes through DNA binding.

We then examined, in vitro and in vivo, the tumor growth rates of WT LMTK3 (MCF7-LMTK3^{WT}) and LMTK3 mutant (MCF7-LMTK3^{RVxF}) cells that lost their DNA binding activity. MCF7-LMTK3^{RVxF} cells proliferated significantly slower compared with MCF7-LMTK3^{WT} cells (Figure 6A). Moreover, mice injected with MCF7-LMTK3^{RVxF} cells also developed smaller tumors compared with WT cells (Figures 6B and 6C). These data indicate that abolishing the DNA binding ability of LMTK3 on tumor suppressor-like genes inhibits tumor progression.

In summary, we propose a model in which nuclear LMTK3 mediates chromatin remodeling by interacting with KAP1 and PP1α (the latter dephosphorylates KAP1 at LMTK3-specific chromatin binding regions, promoting chromatin condensation and transcriptional repression) and tethering the chromatin to the nuclear lamina through interaction with lamin A. These events result in LMTK3 inducing transcriptional repression of its targeted tumor suppressor-like genes and, thereby, supporting cancer cell survival and tumor growth (Figure 7).

DISCUSSION

We have previously demonstrated the role of cytoplasmic LMTK3 in regulating integrin-associated metastatic potential (Xu et al., 2014) and ERα transcriptional activity (Giamas et al., 2011) in breast cancer. Here we describe a role of nuclear LMTK3 and reveal that its chromatin binding and gene regulation are mediated via its scaffold behavior. This is the first time that an RTK has been ascribed such a role, lending credence to

(C) Mapping of LMTK3 directly interacting proteins to constructs of LMTK3 using a GST pull-down assay. Left: schematics of GST-tagged LMTK3 truncation derivatives incubated with whole MCF7 cell lysate and precipitated using a GST antibody. Right: immunoprecipitates tested by western blotting.
(D) The overlap of DamID LADs and LMTK3. The p value was calculated using a genomic association test (GAT) (Heger et al., 2013).
(E) Projections of confocal FISH images with a probe covering LMTK3 distal binding regions in MCF7 and MCF7-LMTK3 cells. FISH signals of the BAC clones RP11-54O14 and RP11-113M21 (non-LMTK3-bound region) are shown.
(F) The percentage of FISH signals at the nuclear periphery is plotted against the H3K9me3 enrichments detected by H3K9me3 ChIP-qPCR within LMTK3-bound distal regions. RP11-113M21 was used as a negative control.
(G and H) Genes were divided into three groups based on their distance to the nearest distal intervals bound by LMTK3. Their expression levels were obtained by RNA-seq analysis.
(I) qPCR of LMTK3 distally bound gene expression in MCF7 and MCF7-LMTK3^{WT} cells.
Quantitative data are presented as mean ± SD. Student's t test was used for statistical analysis. *$p < 0.05$, **$p < 0.01$, ***$p < 0.001$. See also Figure S4.

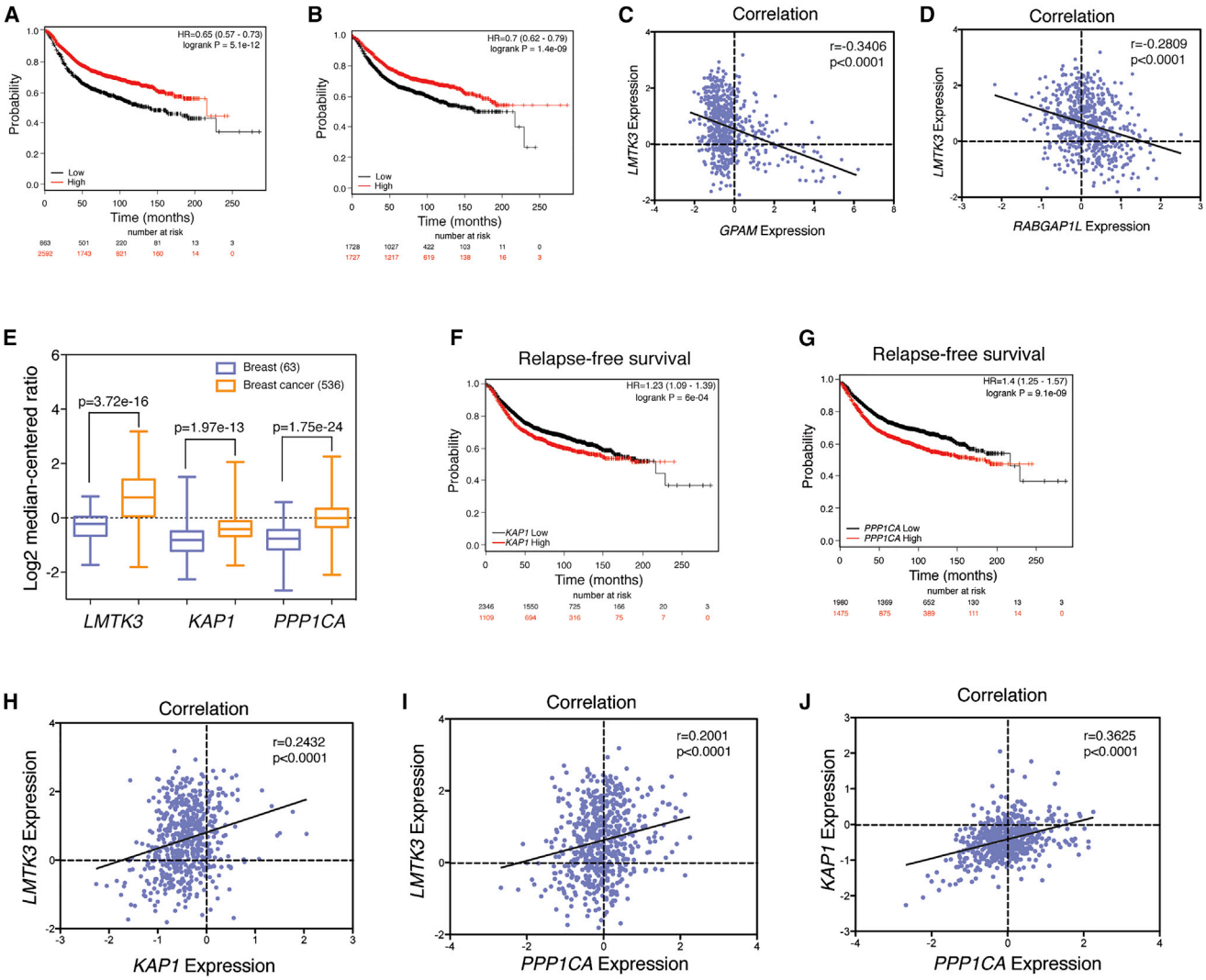

Figure 5. LMTK3, PP1α, and KAP1 Co-express in Breast Cancer and Collaborate in Suppressing the Expression of Tumor Suppressor-like Genes

(A) Kaplan-Meier plots demonstrating the association of the mean expression profile of the available top 30 genes bound by LMTK3 at promoter intervals with relapse-free survival ($p = 5.1 \times 10^{-12}$) in 3,455 breast cancer patients. HR, hazard ratio.

(B) Kaplan-Meier plots demonstrating the association of the mean expression profile of the top ten genes near LMTK3 distal binding intervals with relapse-free survival ($p = 1.4 \times 10^{-9}$) in 3,455 breast cancer patients.

(C and D) Correlation of the expression of *LMTK3* and LMTK3 target genes in TCGA breast cancer datasets. The correlation of *LMTK3* and *GPAM* (C) and *RABGAP1L* (D) is shown as representatives of LMTK3-bound genes at the promoter and distal intervals, respectively.

(E) The expression profiles of *LMTK3*, *KAP1*, and *PPP1CA* in 63 normal breast tissues and 536 breast cancer tissues. Data are presented as mean ± SD. Student's t test was used for statistical analysis.

(F) Kaplan-Meier plots demonstrating the association between *KAP1* expression and relapse-free survival ($p = 6 \times 10^{-4}$) in n = 3455 breast cancer patients.

(G) Kaplan-Meier plots demonstrating the association between *PPP1CA* expression and relapse free survival ($p = 9.1 \times 10^{-9}$) in 3,455 breast cancer patients.

(H–J) Correlation of the expression of *LMTK3*, *KAP1*, and *PPP1CA* in TCGA breast cancer datasets. *LMTK3* and *KAP1* (H), *LMTK3* and *PPP1CA* (I), and *KAP1* and *PPP1CA* (J) are shown.

Kaplan-Meier plots were obtained from http://kmplot.com/. TCGA datasets were obtained from https://tcga-data.nci.nih.gov/tcga/. Correlation statistical analysis was done using Pearson correlation test. See also Figure S5.

the importance of spatial organization in signal propagation. Although scaffolding proteins are typically devoid of catalytic activity, its presence here (by virtue of the fact that it is an active RTK) is likely to have a far greater impact on signal processing that anticipated by its kinase function alone. We propose that this dual function contributes to tumorigenesis by enhancing signaling complexity.

Being an RTK, LMTK3 is unlikely to have a direct DNA binding domain, suggesting the existence of other interacting partners for its chromatin association. We discovered that the

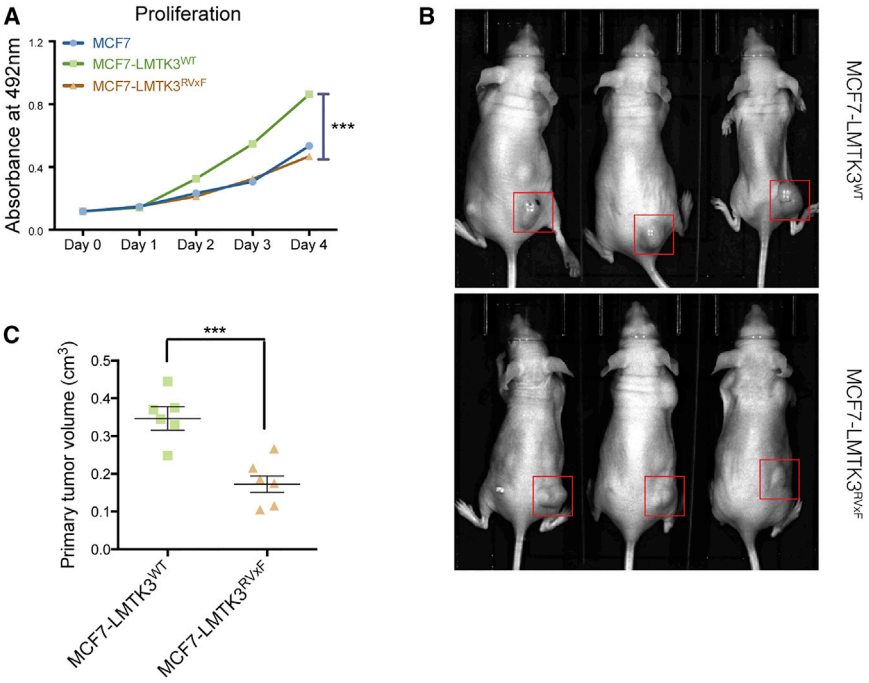

Figure 6. DNA-Binding Activity Is Crucial for LMTK3-Mediated Tumor Growth In Vitro and In Vivo

(A) Sulforhodamine B (SRB) proliferation assay of MCF7-LMTK3^{WT} and MCF7-LMTK3^{RVxF} cells.

(B) Xenografts of BALB/c nude mice subcutaneously injected with MCF7-LMTK3^{WT} and MCF7-LMTK3^{RVxF} cells. Red boxes present the tumors on day 28.

(C) Tumor volumes of xenografts of mice subcutaneously injected with MCF7-LMTK3^{WT} and MCF7-LMTK3^{RVxF} cells on day 14.

Quantitative data are presented as mean ± SD. Student's t test was used for statistical analysis. ***$p < 0.001$. See also Figure S6.

chromatin-binding events of LMTK3 are ERα-independent, and little overlap between the binding genes of LMTK3 and ERα was observed. In addition, ERα was not detected in the RIME analysis. These results appear to be initially contradictory with our previous finding describing LMTK3 as an ERα regulator (as shown by modulating the transcription of *TFF1*, an ERα-regulated gene) (Giamas et al., 2011). However, the binding of LMTK3 and ERα to DNA is an independent procedure. The regulation of ERα by LMTK3 is a transient phosphorylation process that occurs in the cytoplasm, which results in activation of ERα, translocation into the nucleus and binding to specific DNA regions. The process by which LMTK3 itself translocates to the nucleus and interacts with transcription factors (other than ERα), which eventually leads to DNA binding is mediated via other mechanisms, one of which is described here. Therefore, the interaction of LMTK3 with ERα and its phosphorylation at the cytoplasm does not necessarily mean that this complex exists and acts together inside the nucleus and, subsequently, binds to the chromatin.

Therefore, to identify potential partners of LMTK3 in chromatin binding, a RIME assay was employed, and several proteins involved in transcriptional repression were detected, many of which were found to interact with silenced chromatin, and their bindings were associated with enriched H3K9me3 signals (Bartke et al., 2010). Interestingly, only LMTK3 bindings at distal (enhancer) intervals were associated with H3K9me3 enrichment, suggesting a distinct regulation of LMTK3 at promoter and enhancer intervals.

Studies have shown that molecular tethering of H3K9me3-marked heterochromatin to the nuclear periphery results in transcriptional repression of genes located in these regions (Finlan et al., 2008; Reddy et al., 2008; Towbin et al., 2012). Here we demonstrate that LMTK3 functions as a scaffold protein linking heterochromatin to the nuclear lamina. In addition, we show that the expression levels of genes close to LMTK3-bound regions are relatively lower, suggesting that localization to the periphery suppresses the expression of these genes.

Apart from its well defined kinase domain, LMTK3 contains many intrinsically disordered regions (http://www.disprot.org/), which may participate in facilitating protein-protein interactions implicated in a number of cellular processes (Kathiriya et al., 2014; van der Lee et al., 2014). We identified lamin A as a direct interacting partner of LMTK3 that could be at least partly responsible for the tethering process of heterochromatin to the nuclear lamina, which results in chromatin remodeling and H3K9me3 modification and subsequent tumor suppressor-like gene repression. Our model (Figure 7) infers the assembly of an LMTK3 "signalosome," leading to dynamic regulation determined by overall module composition as opposed to individual activity, with subsequent transcriptional effects.

On an evolutionary scale, recombination of catalytic and regulatory or scaffold domains could happen through exon shuffling, and it is probable that a modular architecture is more conducive for the rapid emergence of novel types of regulatory mechanisms. Although it is very difficult to test this argument experimentally, it is interesting to note that organism complexity seems to correlate more with the number and diversity of regulatory domains and not with the number of integrated components (such as catalytic domains) comprising a network (Bhattacharyya et al., 2006). LMTK3 lacks classical scaffolding domain signatures (e.g., protein-protein interaction [PPI] domains such as SH3 and PDZ), but, in common with other scaffolding proteins, it binds signaling molecules both directly and indirectly. Looking at the known examples of known scaffold proteins, it seems that this group of signaling proteins is heterogeneous, and it is unlikely that all scaffolds are linked through a common ancestry. This is supported by the diverse, unrelated ways by which scaffolds can come into existence (e.g., active components turn into scaffolds or scaffolds that form by random associations), and LMTK3 can therefore be categorized as a non-classical, "randomly created" scaffold. The efforts within this study, including genomic ChIP, are necessary to decipher these

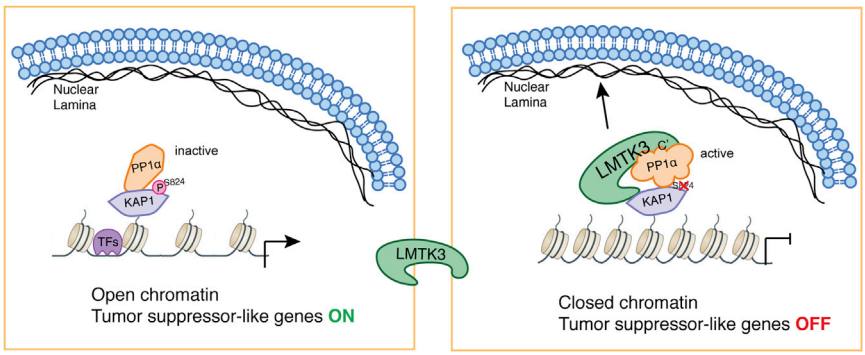

Figure 7. Graphical Summary of Chromatin Remodeling and Transcriptional Corepressor Behavior of LMTK3

A schematic illustration of mechanism of chromatin remodeling mediated by nuclear LMTK3. LMTK3 binds PP1α through its C-terminal domains and interacts with KAP1 and dephosphorylates KAP1 at Ser824, which results in chromatin condensation. Meanwhile, a part of the LMTK3 disordered domain tethers the whole heterochromatin complex to the nuclear lamina through interacting with Lamin A. These result in the transcriptional repression of LMTK3-bound tumor suppressor-like genes.

roles. Unfortunately, comparative genomics, where protein sequences derived from sequenced genomes are compared, has a very low chance to identify scaffolding interactions, and even inferring binary connections between annotated gene products is difficult.

Despite being bound to repressive promoters and enhancers, LMTK3 is also able to bind to active promoters (Figure S1I) via other proteins, among them CREB1. Our LMTK3 ChIP-seq data revealed that the CREB1 motif is one of the most enriched ones. In addition, CREB1 shares binding regions with LMTK3 at the promoters of *PTPN11, PELP1*, and *RPS6KB2*. LMTK3 overexpression promotes the expression of these genes, generally characterized as oncogenes, in breast cancer (Aceto et al., 2012; Pérez-Tenorio et al., 2011; Rajhans et al., 2007; Roy et al., 2012).

KAP1 has been shown to be overexpressed in a number of cancers (Beer et al., 2002; Silva et al., 2006; Yokoe et al., 2010). Here we demonstrate that, when co-expressed with LMTK3, KAP1 functions as an oncogenic transcriptional corepressor through suppressing the expression of a number of tumor suppressor-like genes (Figure 5). KAP1 phosphorylation, especially at Ser824, has been shown to help chromatin decondensation and represents an inhibitory post-translational modification for its co-repressive function (White et al., 2006; Ziv et al., 2006); (Lee et al., 2007); (Li et al., 2007), and its phosphorylation is known to be regulated by the protein phosphatase 1 family members PP1α and PP1β (Li et al., 2010). In our work, we suggest that LMTK3 specifically interacts with PP1α, which suppresses KAP1 phosphorylation at LMTK3-chromatin associated regions, thereby maintaining the co-repressor function of this complex. In addition, KAP1 phosphorylation is a DNA damage marker (White et al., 2006; Ziv et al., 2006). Our results show that KAP1 phosphorylation is suppressed during doxorubicin treatment when LMTK3 is overexpressed, which suggests that LMTK3 abundance might delay the induction of DNA damage upon doxorubicin treatment. However, the contribution of LMTK3 in this process requires further investigation, which might further highlight its role in cancer cell survival.

Collectively, we demonstrate that LMTK3 functions as a transcriptional co-repressor through interacting with PP1α and KAP1 and as a scaffold protein by tethering heterochromatin to the nuclear lamina, resulting in chromatin remodeling and transcriptional repression of LMTK3-bound tumor suppressor-like genes. The idea that an RTK could behave as a scaffold protein opens up potential avenues for future research of these molecules.

EXPERIMENTAL PROCEDURES

Human Primary Tumor Samples

Institutional board approval was obtained for all work on tissue samples in accordance with the Declaration of Helsinki.

Cell Culture and Generation of LMTK3 CRISPR Knockout Cells

Human breast cancer cell lines (MCF7 and MDA-MB-231) were purchased from the American Type Culture Collection and were cultured in DMEM supplemented with 10% fetal calf serum (FCS) and 1% penicillin and streptomycin. Stable LMTK3-expressing MCF7 cells were generated and cultured as described previously (Xu et al., 2014).

For experimental details for the generation of LMTK3 knockout cells, please refer to the Supplemental Experimental Procedures.

ChIP-Seq Analysis

For experimental details, please refer to the Supplemental Experimental Procedures.

Bioinformatic and Statistical Analyses

Peaks were called using model-based analysis for ChIP-seq (MACS) under the following recommended settings: bandwidth, 300; p value cutoff, 1×10^{-5}; mfold range, 10, 30. The false discovery rate (FDR) cutoff was 0.001 (0.1%) for all peaks. Peaks and raw signals were then uploaded to and analyzed with Galaxy and Cistrome.

RIME

RIME was performed as described previously (Mohammed et al., 2013) using an LMTK3 antibody (Abnova, catalog no. H00114783-M02).

FISH

For experimental details, please refer to the Supplemental Experimental Procedures.

Xenograft Mouse Models

BALB/c nude mice 7–8 weeks of age were purchased from Harlan Laboratories UK, and all procedures were carried out under Home Office license authority and local ethics. MCF7-LMTK3^{WT} and MCF7-LMTK3^{RVxF} cells were cultured in DMEM containing 10% FCS and 0.5 mg/ml of G418 and injected subcutaneously into mice (seven mice/group) at a concentration of 5×10^6 cells/mouse. Tumor volumes were measured every 2 days using a caliper.

Public Data Sources

The following ChIP-seq peaks and raw signals were downloaded from the Encyclopedia of DNA Elements (ENCODE): H3K9me3, H3K27me3, H3K27ac, H3K4me1, H3K4me3, Pol2, TAF1, and P300 are generated from MCF7

Please cite this article in press as: Xu et al., LMTK3 Represses Tumor Suppressor-like Genes through Chromatin Remodeling in Breast Cancer, Cell Reports (2015), http://dx.doi.org/10.1016/j.celrep.2015.06.073

cells; SUZ12 and NCOR are generated from K562 cells; and KAP1 is generated from HEK293 cells. ERα peaks and raw signals generated in MCF7 cells were downloaded from a previous publication (Hurtado et al., 2008).

Patient survival data were acquired from http://www.kmplot.com.

Clinical correlation data were acquired from http://www.cbioportal.org and http://www.canevolve.org.

Statistical Analysis

ChIP-seq analyses were done using Galaxy/Cistrome (http://cistrome.org). Other data analyses were performed with Prism. Data are presented as mean ± SD or SEM, as indicated in the figure legends.

ACCESSION NUMBERS

ChIP-seq data reported in this paper have been deposited to the NCBI GEO and are available under accession number GEO: GSE70385. Themass spectrometry proteomics data reported in this paper have been deposited to the ProteomeXchange Consortium (Vizcaíno et al., 2014) and are available under accession number PXD002399.

SUPPLEMENTAL INFORMATION

Supplemental Information includes Supplemental Experimental Procedures, six figures, and two tables and can be found with this article online at http://dx.doi.org/10.1016/j.celrep.2015.06.073.

AUTHOR CONTRIBUTIONS

Y.X., H.Z., L.M., J.S., and G.G. designed the experiments and wrote the manuscript. Y.X., V.T.M.N., H.Z., N.A., and J.N. performed most of the experiments and performed the statistical analysis. A.R. designed the FISH experiments. L.B. designed the CRISPR/CAS9 knockout experiments.

ACKNOWLEDGMENTS

We would like to thank Lei Cheng Lit, Arnhild Grothey, Darren K. Patten, Chao Gao, Andrea Rabitsch, and Inigo Ortiz De Mendibil for technical assistance and helpful discussions. This work was supported by Action Against Cancer and Hilary Craft in particular, Breast Cancer Campaign, Cancer Research UK, and the China Scholarship Council. We would also like to thank Richard and Evelina Girling and the "kinase group" for their support. We give special thanks to The Jaharis Family Foundation, The Rothschild Foundation, Steve Mobbs and Pauline Thomas, and Euromoney plc for their incredible support.

Received: April 23, 2015
Revised: June 11, 2015
Accepted: June 25, 2015
Published: July 23, 2015

REFERENCES

Aceto, N., Sausgruber, N., Brinkhaus, H., Gaidatzis, D., Martiny-Baron, G., Mazzarol, G., Confalonieri, S., Quarto, M., Hu, G., Balwierz, P.J., et al. (2012). Tyrosine phosphatase SHP2 promotes breast cancer progression and maintains tumor-initiating cells via activation of key transcription factors and a positive feedback signaling loop. Nat. Med. *18*, 529–537.

Andrulis, E.D., Neiman, A.M., Zappulla, D.C., and Sternglanz, R. (1998). Perinuclear localization of chromatin facilitates transcriptional silencing. Nature *394*, 592–595.

Bartke, T., Vermeulen, M., Xhemalce, B., Robson, S.C., Mann, M., and Kouzarides, T. (2010). Nucleosome-interacting proteins regulated by DNA and histone methylation. Cell *143*, 470–484.

Beer, D.G., Kardia, S.L., Huang, C.C., Giordano, T.J., Levin, A.M., Misek, D.E., Lin, L., Chen, G., Gharib, T.G., Thomas, D.G., et al. (2002). Gene-expression profiles predict survival of patients with lung adenocarcinoma. Nat. Med. *8*, 816–824.

Bhattacharyya, R.P., Reményi, A., Yeh, B.J., and Lim, W.A. (2006). Domains, motifs, and scaffolds: the role of modular interactions in the evolution and wiring of cell signaling circuits. Annu. Rev. Biochem. *75*, 655–680.

Chubb, J.R., Boyle, S., Perry, P., and Bickmore, W.A. (2002). Chromatin motion is constrained by association with nuclear compartments in human cells. Curr. Biol. *12*, 439–445.

Finlan, L.E., Sproul, D., Thomson, I., Boyle, S., Kerr, E., Perry, P., Ylstra, B., Chubb, J.R., and Bickmore, W.A. (2008). Recruitment to the nuclear periphery can alter expression of genes in human cells. PLoS Genet. *4*, e1000039.

Giamas, G., Filipović, A., Jacob, J., Messier, W., Zhang, H., Yang, D., Zhang, W., Shifa, B.A., Photiou, A., Tralau-Stewart, C., et al. (2011). Kinome screening for regulators of the estrogen receptor identifies LMTK3 as a new therapeutic target in breast cancer. Nat. Med. *17*, 715–719.

Grewal, S.I., and Jia, S. (2007). Heterochromatin revisited. Nat. Rev. Genet. *8*, 35–46.

Guelen, L., Pagie, L., Brasset, E., Meuleman, W., Faza, M.B., Talhout, W., Eussen, B.H., de Klein, A., Wessels, L., de Laat, W., and van Steensel, B. (2008). Domain organization of human chromosomes revealed by mapping of nuclear lamina interactions. Nature *453*, 948–951.

Heger, A., Webber, C., Goodson, M., Ponting, C.P., and Lunter, G. (2013). GAT: a simulation framework for testing the association of genomic intervals. Bioinformatics *29*, 2046–2048.

Hendrickx, A., Beullens, M., Ceulemans, H., Den Abt, T., Van Eynde, A., Nicolaescu, E., Lesage, B., and Bollen, M. (2009). Docking motif-guided mapping of the interactome of protein phosphatase-1. Chem. Biol. *16*, 365–371.

Hung, L.Y., Tseng, J.T., Lee, Y.C., Xia, W., Wang, Y.N., Wu, M.L., Chuang, Y.H., Lai, C.H., and Chang, W.C. (2008). Nuclear epidermal growth factor receptor (EGFR) interacts with signal transducer and activator of transcription 5 (STAT5) in activating Aurora-A gene expression. Nucleic Acids Res. *36*, 4337–4351.

Hurtado, A., Holmes, K.A., Geistlinger, T.R., Hutcheson, I.R., Nicholson, R.I., Brown, M., Jiang, J., Howat, W.J., Ali, S., and Carroll, J.S. (2008). Regulation of ERBB2 by oestrogen receptor-PAX2 determines response to tamoxifen. Nature *456*, 663–666.

Iyengar, S., Ivanov, A.V., Jin, V.X., Rauscher, F.J., 3rd, and Farnham, P.J. (2011). Functional analysis of KAP1 genomic recruitment. Mol. Cell. Biol. *31*, 1833–1847.

Kathiriya, J.J., Pathak, R.R., Clayman, E., Xue, B., Uversky, V.N., and Davé, V. (2014). Presence and utility of intrinsically disordered regions in kinases. Mol. Biosyst. *10*, 2876–2888.

Kind, J., Pagie, L., Ortabozkoyun, H., Boyle, S., de Vries, S.S., Janssen, H., Amendola, M., Nolen, L.D., Bickmore, W.A., and van Steensel, B. (2013). Single-cell dynamics of genome-nuclear lamina interactions. Cell *153*, 178–192.

Kotera, I., Sekimoto, T., Miyamoto, Y., Saiwaki, T., Nagoshi, E., Sakagami, H., Kondo, H., and Yoneda, Y. (2005). Importin alpha transports CaMKIV to the nucleus without utilizing importin beta. EMBO J. *24*, 942–951.

Kumaran, R.I., and Spector, D.L. (2008). A genetic locus targeted to the nuclear periphery in living cells maintains its transcriptional competence. J. Cell Biol. *180*, 51–65.

Lee, Y.K., Thomas, S.N., Yang, A.J., and Ann, D.K. (2007). Doxorubicin down-regulates Kruppel-associated box domain-associated protein 1 sumoylation that relieves its transcription repression on p21WAF1/CIP1 in breast cancer MCF-7 cells. J. Biol. Chem. *282*, 1595–1606.

Li, X., Lee, Y.K., Jeng, J.C., Yen, Y., Schultz, D.C., Shih, H.M., and Ann, D.K. (2007). Role for KAP1 serine 824 phosphorylation and sumoylation/desumoylation switch in regulating KAP1-mediated transcriptional repression. J. Biol. Chem. *282*, 36177–36189.

Li, X., Lin, H.H., Chen, H., Xu, X., Shih, H.M., and Ann, D.K. (2010). SUMOylation of the transcriptional co-repressor KAP1 is regulated by the serine and threonine phosphatase PP1. Sci. Signal. *3*, ra32.

Lin, S.Y., Makino, K., Xia, W., Matin, A., Wen, Y., Kwong, K.Y., Bourguignon, L., and Hung, M.C. (2001). Nuclear localization of EGF receptor and its potential new role as a transcription factor. Nat. Cell Biol. *3*, 802–808.

Lo, H.W., Hsu, S.C., Ali-Seyed, M., Gunduz, M., Xia, W., Wei, Y., Bartholomeusz, G., Shih, J.Y., and Hung, M.C. (2005). Nuclear interaction of EGFR and STAT3 in the activation of the iNOS/NO pathway. Cancer Cell *7*, 575–589.

Meuleman, W., Peric-Hupkes, D., Kind, J., Beaudry, J.B., Pagie, L., Kellis, M., Reinders, M., Wessels, L., and van Steensel, B. (2013). Constitutive nuclear lamina-genome interactions are highly conserved and associated with A/T-rich sequence. Genome Res. *23*, 270–280.

Mohammed, H., D'Santos, C., Serandour, A.A., Ali, H.R., Brown, G.D., Atkins, A., Rueda, O.M., Holmes, K.A., Theodorou, V., Robinson, J.L., et al. (2013). Endogenous purification reveals GREB1 as a key estrogen receptor regulatory factor. Cell Rep. *3*, 342–349.

Nielsen, A.L., Ortiz, J.A., You, J., Oulad-Abdelghani, M., Khechumian, R., Gansmuller, A., Chambon, P., and Losson, R. (1999). Interaction with members of the heterochromatin protein 1 (HP1) family and histone deacetylation are differentially involved in transcriptional silencing by members of the TIF1 family. EMBO J. *18*, 6385–6395.

Peng, H., Moffett, J., Myers, J., Fang, X., Stachowiak, E.K., Maher, P., Kratz, E., Hines, J., Fluharty, S.J., Mizukoshi, E., et al. (2001). Novel nuclear signaling pathway mediates activation of fibroblast growth factor-2 gene by type 1 and type 2 angiotensin II receptors. Mol. Biol. Cell *12*, 449–462.

Pérez-Tenorio, G., Karlsson, E., Waltersson, M.A., Olsson, B., Holmlund, B., Nordenskjöld, B., Fornander, T., Skoog, L., and Stål, O. (2011). Clinical potential of the mTOR targets S6K1 and S6K2 in breast cancer. Breast Cancer Res. Treat. *128*, 713–723.

Peric-Hupkes, D., Meuleman, W., Pagie, L., Bruggeman, S.W., Solovei, I., Brugman, W., Gräf, S., Flicek, P., Kerkhoven, R.M., van Lohuizen, M., et al. (2010). Molecular maps of the reorganization of genome-nuclear lamina interactions during differentiation. Mol. Cell *38*, 603–613.

Pickersgill, H., Kalverda, B., de Wit, E., Talhout, W., Fornerod, M., and van Steensel, B. (2006). Characterization of the Drosophila melanogaster genome at the nuclear lamina. Nat. Genet. *38*, 1005–1014.

Poleshko, A., Mansfield, K.M., Burlingame, C.C., Andrake, M.D., Shah, N.R., and Katz, R.A. (2013). The human protein PRR14 tethers heterochromatin to the nuclear lamina during interphase and mitotic exit. Cell Rep. *5*, 292–301.

Rajhans, R., Nair, S., Holden, A.H., Kumar, R., Tekmal, R.R., and Vadlamudi, R.K. (2007). Oncogenic potential of the nuclear receptor coregulator proline-, glutamic acid-, leucine-rich protein 1/modulator of the nongenomic actions of the estrogen receptor. Cancer Res. *67*, 5505–5512.

Reddy, K.L., Zullo, J.M., Bertolino, E., and Singh, H. (2008). Transcriptional repression mediated by repositioning of genes to the nuclear lamina. Nature *452*, 243–247.

Roux, K.J., Kim, D.I., Raida, M., and Burke, B. (2012). A promiscuous biotin ligase fusion protein identifies proximal and interacting proteins in mammalian cells. J. Cell Biol. *196*, 801–810.

Roy, S., Chakravarty, D., Cortez, V., De Mukhopadhyay, K., Bandyopadhyay, A., Ahn, J.M., Raj, G.V., Tekmal, R.R., Sun, L., and Vadlamudi, R.K. (2012). Significance of PELP1 in ER-negative breast cancer metastasis. Mol. Cancer Res. *10*, 25–33.

Ryan, R.F., Schultz, D.C., Ayyanathan, K., Singh, P.B., Friedman, J.R., Fredericks, W.J., and Rauscher, F.J., 3rd. (1999). KAP-1 corepressor protein interacts and colocalizes with heterochromatic and euchromatic HP1 proteins: a potential role for Krüppel-associated box-zinc finger proteins in heterochromatin-mediated gene silencing. Mol. Cell. Biol. *19*, 4366–4378.

Sadaie, M., Salama, R., Carroll, T., Tomimatsu, K., Chandra, T., Young, A.R., Narita, M., Pérez-Mancera, P.A., Bennett, D.C., Chong, H., et al. (2013). Redistribution of the Lamin B1 genomic binding profile affects rearrangement of heterochromatic domains and SAHF formation during senescence. Genes Dev. *27*, 1800–1808.

Silva, F.P., Hamamoto, R., Furukawa, Y., and Nakamura, Y. (2006). TIPUH1 encodes a novel KRAB zinc-finger protein highly expressed in human hepatocellular carcinomas. Oncogene *25*, 5063–5070.

Solovei, I., Wang, A.S., Thanisch, K., Schmidt, C.S., Krebs, S., Zwerger, M., Cohen, T.V., Devys, D., Foisner, R., Peichl, L., et al. (2013). LBR and lamin A/C sequentially tether peripheral heterochromatin and inversely regulate differentiation. Cell *152*, 584–598.

Stebbing, J., Filipovic, A., Ellis, I.O., Green, A.R., D'Silva, T.R., Lenz, H.J., Coombes, R.C., Wang, T., Lee, S.C., and Giamas, G. (2012). LMTK3 expression in breast cancer: association with tumor phenotype and clinical outcome. Breast Cancer Res. Treat. *132*, 537–544.

Stebbing, J., Filipovic, A., Lit, L.C., Blighe, K., Grothey, A., Xu, Y., Miki, Y., Chow, L.W., Coombes, R.C., Sasano, H., et al. (2013). LMTK3 is implicated in endocrine resistance via multiple signaling pathways. Oncogene *32*, 3371–3380.

Towbin, B.D., González-Aguilera, C., Sack, R., Gaidatzis, D., Kalck, V., Meister, P., Askjaer, P., and Gasser, S.M. (2012). Step-wise methylation of histone H3K9 positions heterochromatin at the nuclear periphery. Cell *150*, 934–947.

van der Lee, R., Buljan, M., Lang, B., Weatheritt, R.J., Daughdrill, G.W., Dunker, A.K., Fuxreiter, M., Gough, J., Gsponer, J., Jones, D.T., et al. (2014). Classification of intrinsically disordered regions and proteins. Chem. Rev. *114*, 6589–6631.

Vizcaíno, J.A., Deutsch, E.W., Wang, R., Csordas, A., Reisinger, F., Ríos, D., Dianes, J.A., Sun, Z., Farrah, T., Bandeira, N., et al. (2014). ProteomeXchange provides globally coordinated proteomics data submission and dissemination. Nat. Biotechnol. *32*, 223–226.

Vogel, M.J., Guelen, L., de Wit, E., Peric-Hupkes, D., Lodén, M., Talhout, W., Feenstra, M., Abbas, B., Classen, A.K., and van Steensel, B. (2006). Human heterochromatin proteins form large domains containing KRAB-ZNF genes. Genome Res. *16*, 1493–1504.

Wang, S.C., Lien, H.C., Xia, W., Chen, I.F., Lo, H.W., Wang, Z., Ali-Seyed, M., Lee, D.F., Bartholomeusz, G., Ou-Yang, F., et al. (2004). Binding at and transactivation of the COX-2 promoter by nuclear tyrosine kinase receptor ErbB-2. Cancer Cell *6*, 251–261.

Weis, K. (2003). Regulating access to the genome: nucleocytoplasmic transport throughout the cell cycle. Cell *112*, 441–451.

White, D.E., Negorev, D., Peng, H., Ivanov, A.V., Maul, G.G., and Rauscher, F.J., 3rd. (2006). KAP1, a novel substrate for PIKK family members, colocalizes with numerous damage response factors at DNA lesions. Cancer Res. *66*, 11594–11599.

Xu, Y., Zhang, H., Lit, L.C., Grothey, A., Athanasiadou, M., Kiritsi, M., Lombardo, Y., Frampton, A.E., Green, A.R., Ellis, I.O., et al. (2014). The kinase LMTK3 promotes invasion in breast cancer through GRB2-mediated induction of integrin β_1. Sci. Signal. *7*, ra58.

Yokoe, T., Toiyama, Y., Okugawa, Y., Tanaka, K., Ohi, M., Inoue, Y., Mohri, Y., Miki, C., and Kusunoki, M. (2010). KAP1 is associated with peritoneal carcinomatosis in gastric cancer. Ann. Surg. Oncol. *17*, 821–828.

Zeng, W., Ball, A.R., Jr., and Yokomori, K. (2010). HP1: heterochromatin binding proteins working the genome. Epigenetics *5*, 287–292.

Ziv, Y., Bielopolski, D., Galanty, Y., Lukas, C., Taya, Y., Schultz, D.C., Lukas, J., Bekker-Jensen, S., Bartek, J., and Shiloh, Y. (2006). Chromatin relaxation in response to DNA double-strand breaks is modulated by a novel ATM- and KAP-1 dependent pathway. Nat. Cell Biol. *8*, 870–876.

Cell Reports

Supplemental Information

LMTK3 Represses Tumor Suppressor-like Genes through Chromatin Remodeling in Breast Cancer

Yichen Xu, Hua Zhang, Van Thuy Mai Nguyen, Nicos Angelopoulos, Joao Nunes, Alistair Reid, Laki Buluwela, Luca Magnani, Justin Stebbing, and Georgios Giamas

SUPPLEMENTAL DATA

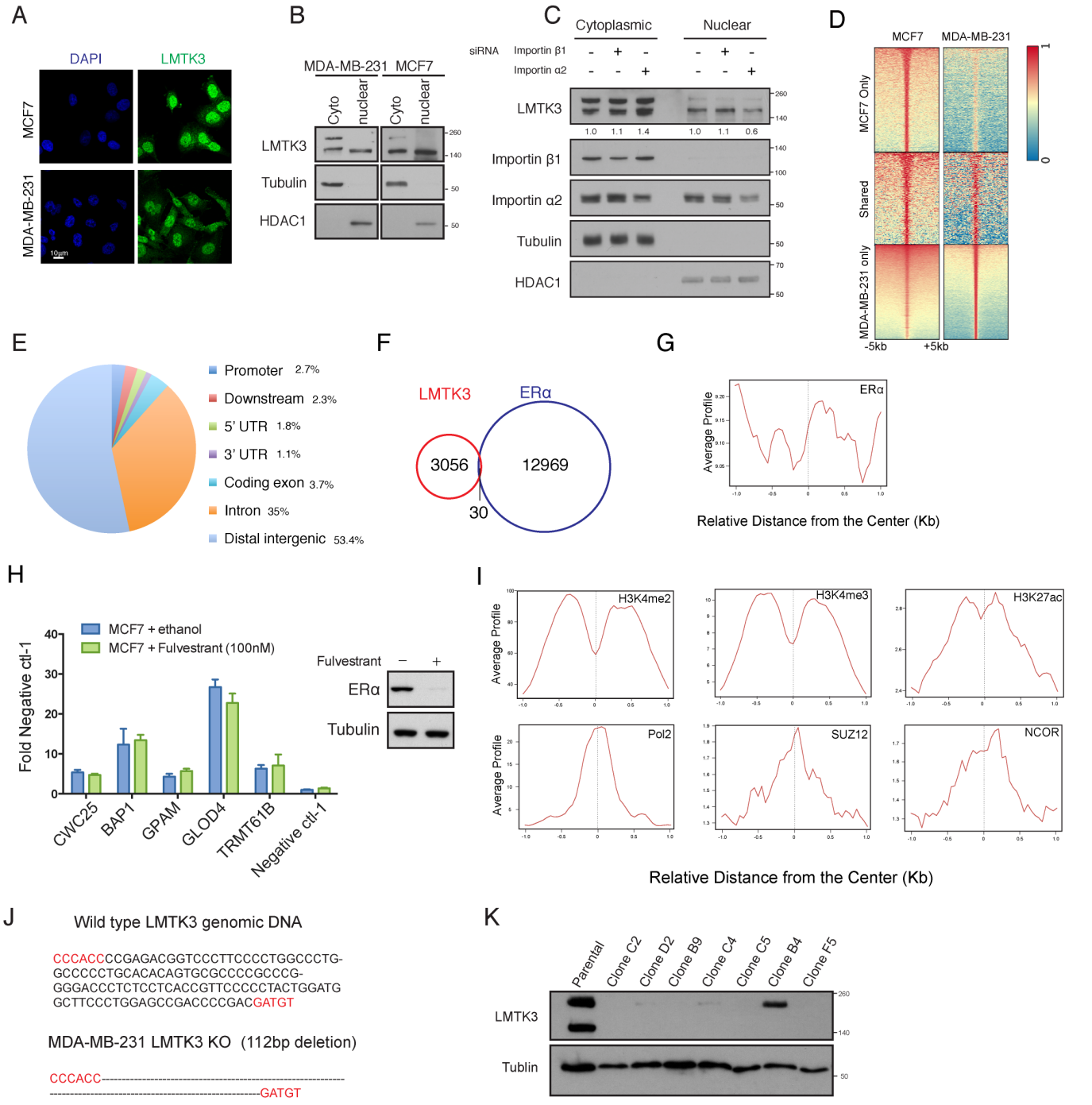

Figure S1, related to Figure 1. Genome-wide bindings of LMTK3 in MCF7 and MDA-MB-231 cells are highly associated and ERα-independent.

(A) Immunofluorescence staining of LMTK3 in MCF7 and MDA-MB-231 breast cancer cells. (B, C) Western blotting of LMTK3 in cytoplasmic and nuclear cell fractions of MDA-MB-231 and MCF7 cells (B), and MDA-MB-231 cells transfected with Importin β1 and Importin α2 siRNAs for 72 hr (C). (D) Heat map showing LMTK3 binding events in MCF7 and MDA-MB-231 cells. (E) Distributions of LMTK3 binding events in MCF7. (F) Venn diagram presenting the overlap of LMTK3 and ERα binding events in MCF7. (G) LMTK3 enrichments around ERα peaks in MCF7 cells. (H) LMTK3 ChIP-qPCR of MCF7 cells treated with 100nM fulvestrant or ethanol for 48 hr. Western blot for ERα was shown. (I) H3K4me2, H3K4me3, H3K27ac, Pol2, SUZ12 and NCOR enrichments around LMTK3 peaks. (J) Genomic DNA sequence of CRISPR targeting site in MDA-MB-231 LMTK3 KO cell clones. 112bp deletion was detected. (K) Western blotting of selected clones.

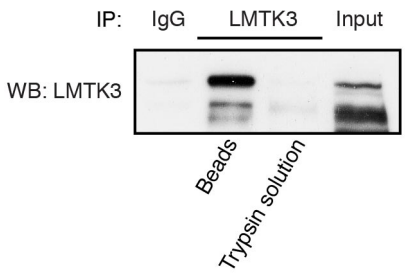

Figure S2, related to Figure 2. RIME validation.
LMTK3 and its interacting proteins were precipitated using LMTK3 antibody, and then trypsinized overnight. Beads and trypsin solution were eluted with 2x laemmli buffer, and western blotting results were shown.

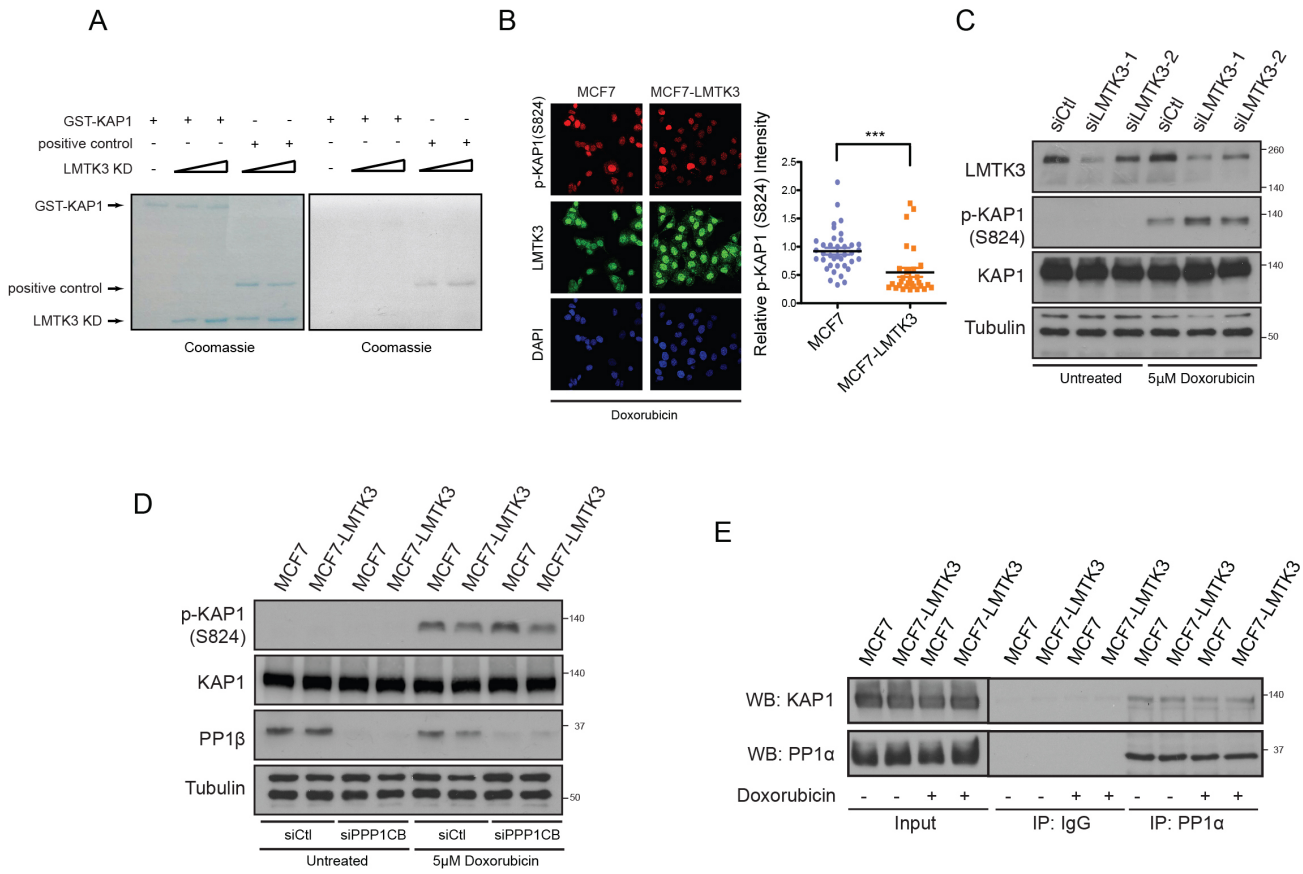

Figure S3, related to Figure 3. LMTK3 suppresses KAP1 Ser824 phosphorylation through PP1α but not PP1β.

(A) *in vitro* kinase assay testing LMTK3 kinase domain (KD) phosphorylation on KAP1 and positive control (B) Immunofluorescence staining of phosphor-KAP1 (S824) and LMTK3 in MCF7 and MCF7-LMTK3 cells treated with doxorubicin for 1 hr. Quantification of relative phosphor-KAP1 intensity is shown. Student's t test was used for statistical analysis. ***p < 0.001. (C) Western blotting of indicated proteins in MCF7-LMTK3 cells restored with *LMTK3* siRNAs treated with doxorubicin for 1 hr. (D) Western blotting of indicated proteins in MCF7 and MCF7-LMTK3 cells transfected with *PPP1CB* siRNA for 72 hr and treated with doxorubicin for 1 hr. (E) Immunoprecipitation of KAP1 with PP1α in MCF7 and MCF7-LMTK3 lysates.

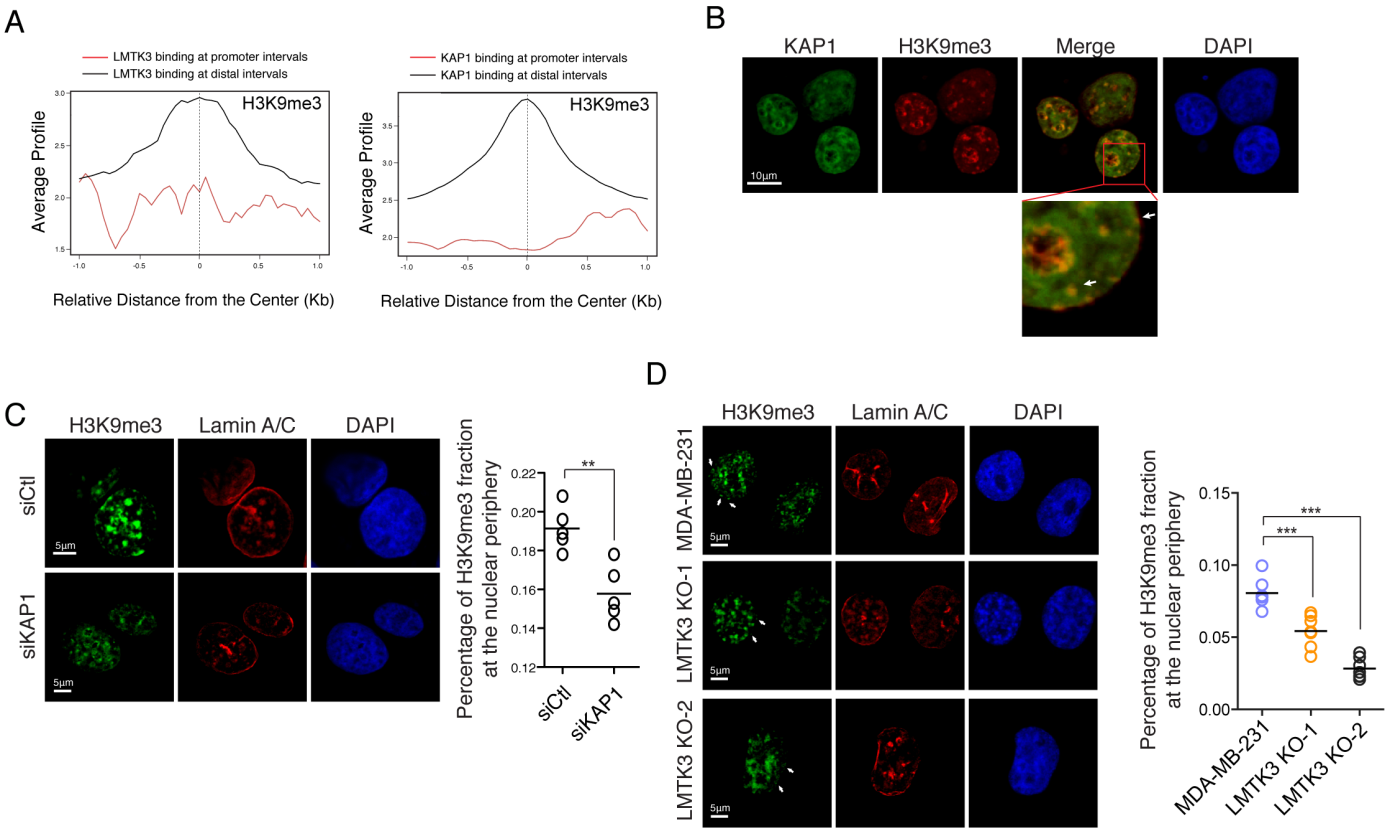

Figure S4, related to Figure 4. LMTK3 and KAP1 regulate the heterochromatin tethering process.

(A) H3K9me3 signal profiles around the promoter (red) and the distal (black) intervals bound by LMTK3 (left panel) and KAP1 (right panel). (B) Confocal staining of KAP1 and H3K9me3 in MCF7. (C) Confocal staining of H3K9me3 and Lamin A/C in MCF7 cells with KAP1 silencing for 72 hr. H3K9me3 signals at the nuclear periphery were quantified. (D) Confocal staining of H3K9me3 and Lamin A/C in MDA-MB-231 cells and LMTK3 KO MDA-MB-231 cells. H3K9me3 signals at the nuclear periphery were quantified. Student's t test was used for statistical analysis. **p < 0.01, ***p < 0.001.

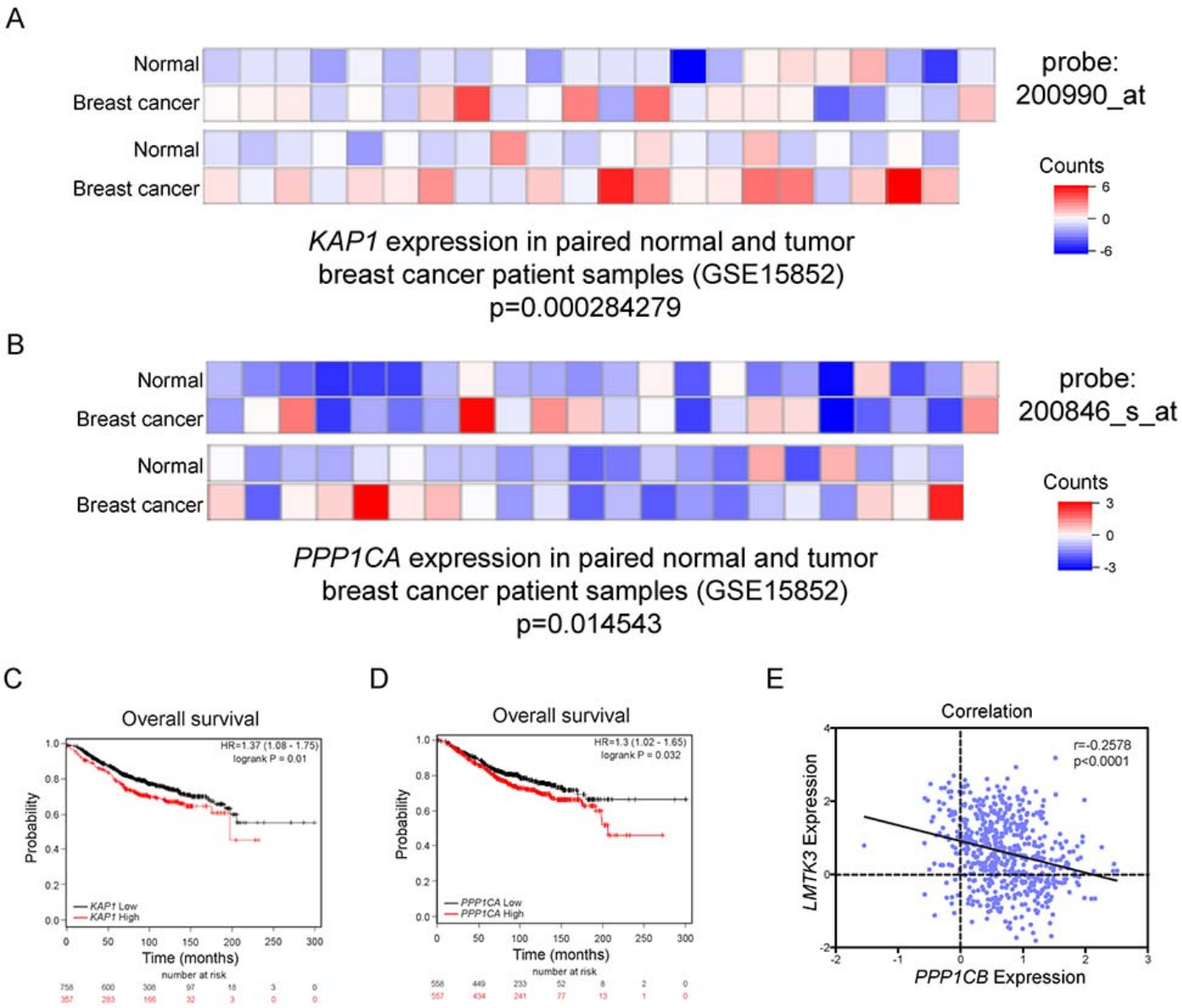

Figure S5, related to Figure 5. PP1α and KAP1 are overexpressed in breast cancer and associated with poorer overall survival.

(A, B) Heat maps of *KAP1* (A) and *PPP1CA* (B) expressions in 43 paired normal and breast cancer tissues, obtained from http://canevolve.org based on GSE15852. (C, D) Kaplan-Meier plots demonstrating the association between *KAP1* expression (C) and *PPP1CA* (D) and overall survival in n=1115 breast cancer patients. (E) Correlation of the expressions of *LMTK3* and *PPP1CB* in TCGA breast cancer datasets. Correlation statistical analysis was done using the Pearson Correlation test.

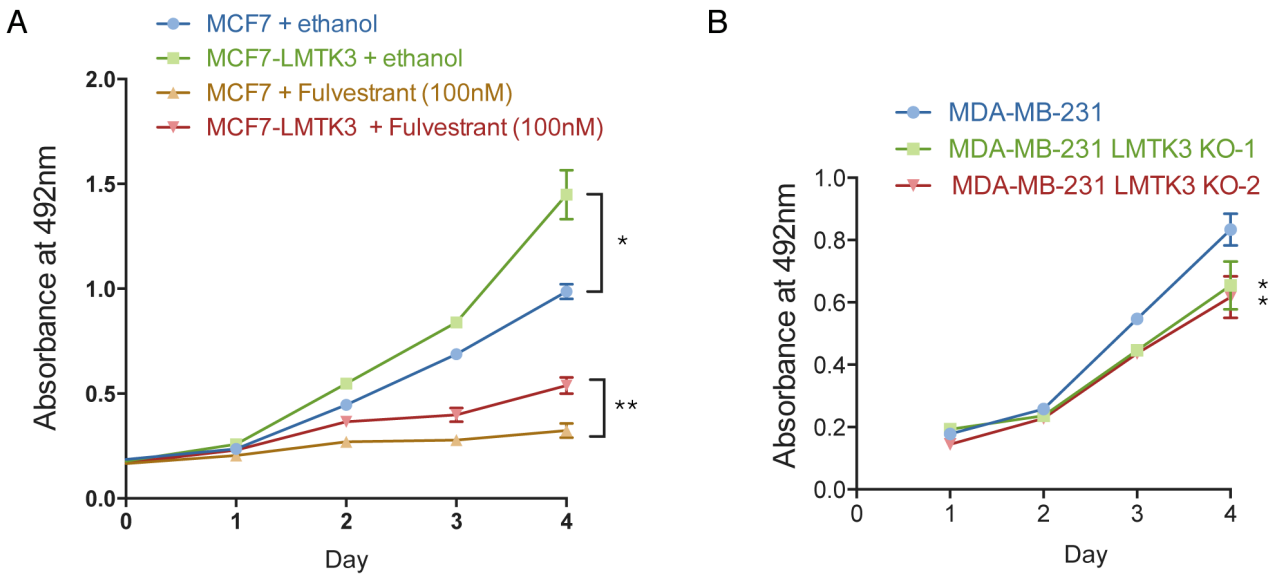

Figure S6, related to Figure 6. LMTK3 can stimulate cell proliferation without the presence of ERα.

(A) Proliferation of MCF7 and MCF7-LMTK3 cells treated with 100nM fulvestrant or ethanol. Percentage reductions of cell viability of MCF7 and MCF7-LMTK3 cells after treating with fulvestrant were calculated. (B) Proliferation of MDA-MB-231 and LMTK3 KO clones (KO-1 and KO-2) cells.

Table S1, related to Figure 2. LMTK3-associated proteins on chromatin detected by RIME, Gene IDs are shown.

AHNK	*DDX5*	*FXR1*	*HS90B*	*NHRF1*	*RBM14*	*RS16*	*SYFA*
ALDOA	*DDX6*	*FXR2*	*HSP71*	*NONO*	*RBM3*	*RS17L*	*TADBP*
ANXA2	*DHX36*	*G3BP1*	*IF4A1*	*NOP16*	*RBM4*	*RS2*	*TBA1A*
ATX2	*DHX9*	*G3BP2*	*IF4B*	*NOP58*	*RBM47*	*RS24*	*TBB4B*
ATX2L	*DYHC1*	*G3P*	*IF4G1*	*NP1L1*	*RBMX*	*RS26*	*TCP4*
BAF	*EF1A2*	*GEMI5*	*IF4H*	*NUCL*	*RENT1*	*RS28*	*TCPZ*
CAPR1	*EF1B*	*GRSF1*	*ILF2*	*PABP1*	*RL11*	*RS3*	*THOC4*
CAZA1	*EF1D*	*H13*	*ILF3*	*PAIRB*	*RL12*	*RS3A*	*TIAR*
CBX3	*EF1G*	*H2A1B*	*IMA2*	*PATL1*	*RL18*	*RS6*	*TIF1B*
CC124	*EF2*	*H2AY*	*KHDR1*	*PCBP2*	*RL19*	*RS7*	*TKT*
CCDC9	*EIF3A*	*H2B1B*	*KPYM*	*PDE3B*	*RL23A*	*RS8*	*TRI25*
CDV3	*EIF3C*	*H31T*	*LAP2A*	*PGK1*	*RL27A*	*RTCB*	*UBP10*
CIRBP	*ELAV1*	*H4*	*LARP1*	*PLEC*	*RL3*	*SERA*	*UBP2L*
CLIC1	*ENOA*	*HMGB1*	*LARP4*	*PPIA*	*RL38*	*SF3B2*	*WIBG*
CO3	*ERF1*	*HNRH1*	*LMNA*	*PRC2A*	*RL4*	*SFPQ*	*XRCC6*
COF1	*ERF3A*	*HNRH3*	*LMNB1*	*PRDX1*	*RL6*	*SND1*	*YBOX2*
CPSF6	*ESRP1*	*HNRL2*	*LRC47*	*PRDX2*	*RL7A*	*SRC8*	*YTHD2*
CRIP2	*F120A*	*HNRPD*	*LS14B*	*PRDX6*	*ROA0*	*SRP14*	*YTHD3*
CSDE1	*FAS*	*HNRPF*	*MATR3*	*PROF1*	*ROA1*	*SRRM2*	*ZC3H8*
DAZP1	*FLNA*	*HNRPK*	*MBNL1*	*PSPC1*	*ROA2*	*SRSF2*	*ZN131*
DBPA	*FMR1*	*HNRPL*	*MIF*	*PTBP1*	*ROA3*	*SRSF3*	*ZN326*
DD19A	*FUBP1*	*HNRPQ*	*MK67I*	*PUM1*	*ROAA*	*SRSF6*	
DDX1	*FUBP2*	*HNRPR*	*MOV10*	*PUR9*	*RRMJ3*	*SRSF9*	
DDX17	*FUBP3*	*HNRPU*	*MYEF2*	*PURA*	*RS10*	*STAU1*	
DDX3X	*FUS*	*HS90A*	*NEDD8*	*RAN*	*RS14*	*STAU2*	

Table S2. Primers used in this study.

	Gene names	F’	R’
Genomic DNA	*BAP1*	CCTCAGTCCCACACACAGAC	GGAAGACGAGCCCAGAGG
	GLOD4	CTGCGAGCAGCCATGATT	CGCCATGTTCCCTGAGAC
	GPAM	AGTTCGCACCCTAGCAGCTC	CGCACACTCGAGTACACACA
	RBM42	CTCATAGGCCCAGGTTCTTG	CCGCTGGTTCTGCTGTCTAC
	TRMT61B	AGGCACAGCAAGACAGGAC	GGATGGTCACTCAACCAGGA
	CWC25	GAAATAGTTCGGGGGCTACC	AGCCCTGTACGTCATCGTTC
	C1D	GACTCCAGTCTCCCGGAAAG	TGAGATTTGCCTTTGGAGAAG
	Distal-1	AAAGAGACAGCAGCCAGAGG	GAGCACTACCTCGCACACTG
	Distal-2	TCCCTACGTGGGTAATCTGG	CACAGCCACTGAGTGAAGGA
	Distal-3	GTTGTCTGGGATGTGCATTG	ACACAGTGGGGTCACAGATG
	Negative ctl-1	GAGCAGCATTTTAGGCTTGG	TGCAGTGGCTTTTCTCAATG
	Negative ctl-2	AAACCTGCACGCTGGACTAC	CATGGCTGGCAAGAAGGT
cDNA	*CWC25*	ATTCCTCCCCTGTTTTGTCC	GAAGACCCTGGTTACGGTCA
	GLOD4	AGATTCTGACTCCCCTGGTG	GCTTCCCTCTGGATCCATCT
	GPAM	CCAGCCTGTGCTACCTTCTC	CTGTTTCATGGCAGACTTGG
	RBM42	CTGTGATCCGCCCAATTATC	CCACCATGGGAGGAACTACT
	TRMT61B	CCCAGGTGATACTGTTTTGGA	GCCAGATCATGGTGGTCTTT
	TFPT	CGGGAATTAAATCGCAGAAA	CCGAGTTATCCTCTGCACCT
	RNFT2	CGAATGCCTACCTCCAGTGT	TGGAATGTTATCCGTGTTGC
	C12orf49	GCTGCAGCGCCTATGAGTA	CCAGGCACAACTCAAAGTGA
	HRK	GGCCTTTCTTGTGCTTTTGA	TCATACCCATCCTCCTCCAG
	RABGAP1L	GGATCATCTGATTCTGTGGCTA	CTCTTCCATGGCTTTTTCCA
	KIF5C	CAGCAGGAGGTGGATCGTAT	GAGATGAGGCCGGGTAGTGT
	PIP4K2A	CAGTGGAGCTCGTTTTCACA	GAAGAAGGGTGATCCCATGA

SUPPLEMENTAL EXPERIMENTAL PROCEDURES

Generation of LMTK3 CRISPR knockout cells

MDA-MB-231 cells were transiently cotransfected with expression plasmids encoding the CRISPR guide RNA pairs (gRNA_1: GTGACCGTGAGCACATCGTC, gRNA_2: GGAAGGGACCGTCTCGGGGT) against LMTK3 exon 12, together with an expression plasmid encoding a CAS9-GFP fusion protein (Addgene), using lipofectamine LTX (Invitrogen, Carlsbad, CA). 72 hr following transfection, cells were FACS sorted for GFP expression and re-plated at clonal densities to obtain single-cell clones. Genomic DNA from individual clones was used in PCR analysis of LMTK exon 12 and products indicating CRIPSR mediated deletion within the exon further characterized by DNA sequencing. Cell lysates prepared from LMTK3 exon 12 deletion positive clones were used in western blot analysis to confirm LMTK3 knockout.

Chromatin immunoprecipitation (ChIP) and coupled to deep sequencing (ChIP-seq) analysis

ChIP was performed with LMTK3 antibody (Abnova H00114783-M02). The sequences of primers used in ChIP-qPCR are listed in Supplemental Table S1. Negative control primers are targeting the chromatin regions that are not associated with LMTK3.

For generating the ChIP-seq library, 5 ng of LMTK3 ChIP-enriched DNA was modified with the ChIP-seq DNA Sample Prep Kit (Illumina). The DNA end was ligated with adaptor (NEBNext® Multiplex Oligos for Illumina (Index Primers Set 1)), and PCR amplified for 15 rounds. Amplified DNA was gel purified through collecting the fragments around 300bp. The purified DNA was sent for sequencing (Illumina). Sequences were mapped to the human genome (hg19) using BOWTIE to yield unique alignments. Mapping rates are 90.24% and 88.38% for MCF7 and MDA-MB-231, respectively.

Quantitative Real-time PCR

RNA was harvested using RNeasy Kit (Qiagen) and 1µg of RNA was reverse-transcribed to cDNA (complementary DNA) using High Capagcity cDNA Reverse Transcription Kit (Applied Biosystems, Life Technologies). qRT-PCR was performed using SYBR Green assays (Applied Biosystems). For primers used in this study, *BAP1* (QT00204701) and *C1D* (QT00041475) were purchased from Qiagen, the rest refer to Supplemental Table S2.

Immunofluorescence

MCF7 cells were seeded on coverslips and fixed for 15 min using 4% formaldehyde for 10 min, followed by incubation in 0.2% Triton X-100 for 10 min. Cells were then incubated with primary antibody (Mouse LMTK3 (Abnova H00114783-M02), 1:200; Mouse KAP1 (Abcam ab22553), 1:500; Rabbit Lamin A (Abcam ab2630), 1:1000; Mouse Lamin A/C (Santa Cruz sc-7292), 1:400; Rabbit H3K9me3 (Abcam ab8899), 1:500, Rabbit KAP1 (phospho S824) (Abcam ab70369), 1:1000) for 2 hr at room temperature. Subsequently, cells were washed with PBS and incubated with FITC (fluorescein isothiocyanate) or Texas Red–conjugated secondary antibodies for 1 hr each at room temperature. After being washed three times in PBS and air-dried, the coverslips were mounted in ProLong Gold anti-fade reagent with DAPI (Invitrogen, Carlsbad, CA). Fluorescence was detected using a Leica SP5 Confocal Microscope at appropriate wavelengths.

Fluorescence In Situ Hybridization (FISH)

MCF7 and MCF7-LMTK3 cell pellets were resuspended and incubated with hypotonic solution for 15 min at 37°C, followed by 5 min centrifuging at 1300 rpm. Cells were fixed and a drop of the cells were placed on the slide, followed by 37°C incubation overnight. Slides were supplied with 150-200 µl of 0.005% Pepsin/0.001 M HCl and incubated for 15 min at 37°C. Slides were incubated in PBS for 5 min, post fixation washing buffer (10% PBS (10x), 10% $MgCl_2$ 0.5M in H_2O) for 5 min, Paraformaldehyde (PFA) /PBS (10% PBS (10x), 10% $MgCl_2$ 0.5M, 30% H_2O and 50% of 8% PFA) for

5 min, PBS for 5min and 5 min each in ethanol series (70%, 90%, 100%). Slides were air-dried and supplied with the hybridization mix (1µl of indicated probes, 4.5 µl of pure formamide, 3.6 µl 25% Dextran Solfate and 0.9 µl of 20x SSC solution), followed by 5 min incubation at 75°C and 37°C overnight in dark. Slides were washed three times with 0.1x SSC for 5 min each at 57°C. Slides were supplied with DAPI and ready for analysis under the confocal microscope.

Western blotting, immunoprecipitation and GST-pull-down assay.

Cells were lysed in RIPA buffer (#R0278, SIGMA-ALDAICH) or co-IP buffer (for immunoprecipitation; 50mM Tris pH 8.0, 150 mM NaCl, 0.5% Triton X- 100, 10% Glycerol, 1mM DTT) supplemented with protease and phosphatase inhibitors. Cell lysates were resolved by SDS–PAGE and immunoblotted with indicated antibodies. For immunoprecipitation, indicated antibodies (2 µg) were incubated with beads (ImmunoCruz™ IP/WB Optima Systems) for 2 hr at 4 °C, followed by three times wash with PBS. Beads and antibodies were then incubated with 1 mg of cell lysates at 4 °C overnight. Immunoprecipitates were washed three times with co-IP buffer before being resolved by SDS–PAGE and immunoblotted with indicated antibodies. For GST-pull-down assay, 20 µg GST-tagged proteins were incubated with GST beads 2 hr at 4 °C, followed by three times wash with PBS. 1mg cell lysates harvested by RIPA buffer were then incubated with beads at 4 °C overnight, followed by five times washing with PBS and then resolved by SDS–PAGE and immunoblotted with indicated antibodies.